Scattering of flexural waves by multiple narrow cracks in ice sheets floating on water

R. Porter & D.V. Evans

School of Mathematics, University of Bristol, Bristol, BS8 1TW, UK.

October 12, 2004

Abstract

An explicit solution is derived for the reflection and transmission of flexural-gravity waves propagating on a uniform elastic ice sheet floating on water which are obliquely-incident upon any number, N, of narrow parallel cracks of arbitrary separation. The solution is expressed in terms of a system of $2N$ linear equations for the jumps in the displacements and gradients across each of the cracks. A number of interesting features of the problem are addressed including the scattering by periodically-spaced arrays of cracks, the existence of localised edge wave solutions which travel along each of the cracks and examples of non-uniqueness, or trapped waves, in the case of four cracks. The problem of wave reflection by a semi-infinite periodic array of cracks is also formulated exactly in terms of a convergent infinite system of equations and relies on certain properties of the so-called Bloch problem for wave propagation through infinite periodic array of cracks.

1 Introduction

In a recent paper (Evans & Porter 2003, hereafter referred to as EP) the authors derived an explicit solution for the motion of flexural-gravity waves on the surface of ice sheets which contained an infinitely-long straight-line narrow crack. The edges of the ice sheets, which were modelled as thin elastic plates, were free to move and the water on which they rested was of finite depth. By taking advantage of the symmetry of the geometry, simple expressions were obtained for the reflection and transmission coefficients when a wave is obliquely-incident on the crack from infinity. Also, it was shown that for certain frequencies, there existed symmetric *edge waves* which are characterised by a localised wave propagating in the direction of the crack but which does not radiate energy in a direction perpendicular to the crack. The method of solution provided considerable simplification over previous approaches, many of which were reviewed in EP and to which the reader is referred.

In the present paper we investigate whether the method of EP can be extended to the scattering of an obliquely-incident wave by any number, N say, of parallel cracks having arbitrary spacing between them. This problem has an application to the study of the marginal ice zone in the antarctic, located at the interface between shore fast sea-ice and the open sea, where the stresses induced in the ice by the incident waves can break up ice sheets into long rectangular strips (Squire *et al* (1995)).

The multiple crack problem appears to have received little attention, but a notable exception is the work of Squire & Dixon (2001) who extend their treatment of the single crack problem in deep water utilising an appropriate Green's function in the fluid to express the solution in terms of the jumps in the displacements Q_j and slopes P_j, $j = 1, 2, \ldots, N$ of the elastic plates at each crack. These quantities are in turn determined as the $2N$ roots of an inhomogeneous linear set of algebraic equations.

Our approach differs significantly from that of Squire of Dixon (2001) and provides a more direct and straightforward solution without the need to introduce Green's functions. Indeed, it also provides new insight to the solution to the single crack problem considered in EP. Thus we introduce, in section 2.2 below, a pair of canonical single-crack source functions from which the full solution for N arbitrarily-spaced cracks may be constructed. These functions, in addition to satisfying the required field and boundary conditions also satisfy certain jump conditions on their derivatives across the crack position which provide a forcing which radiates waves to infinity. Each of the two single crack source functions may be defined in terms of certain combinations of derivatives of the solution to a single fundamental problem which simply involves a delta-function forcing on the elastic plate and whose explicit solution is readily obtained using Fourier transforms in terms of a rapidly convergent infinite series. Similar ideas were used by Leppington (1978) in a problem involving pinned elastic plates coupled to an acoustic medium, although the boundary conditions in this case are much more straightforward to consider than in our case where the edges of the cracks are free to move. An appropriate linear combination of the single crack functions involving P_j and Q_j for $j = 1, 2, \ldots, N$, introduced in section 2.3 below, is easily shown to satisfy all the conditions for the scattering of an incident wave by N arbitrarily-spaced cracks. For $N = 1$ the method provides a simplification of the analysis leading to the solution in EP.

In addition to calculating the reflection and transmission coefficients for wave scattering by any number of cracks, a number of other aspects of the problem are addressed. These include the existence of edge waves of different frequencies depending on the number of cracks, the condition for which is simply the requirement that the determinant of the $2N$ by $2N$ system of equations vanishes; the existence of zeros of transmission by two closely-spaced cracks which is shown to lead to trapped modes in the case of two pairs of cracks; the existence of a Bloch coefficient μ which determines stopping and passing bands in the case of an infinite number of equally-spaced cracks extending indefinitely throughout the ice sheet; the part played by μ in modifying the theory for scattering by N cracks to derive a convergent system describing the scattering by a semi-infinite periodic array of cracks, and the development of a wide-spacing approximation to many of the above problems. Rather than give a detailed account of each of these problems at this point in the paper, we shall introduce them and related references to the literature in the appropriate part of the paper.

The outline of the paper is as follows. In the long section 2 the problem of the scattering of incident waves by N arbitrarily-spaced cracks is formulated and solved. The solution of this problem provides the platform for many of the subsequent sections. The essential results are encapsulated in the equations (2.54) and (2.55) whose solutions are Q_j, P_j for $j = 1, 2, \ldots, N$, the jumps in the displacements and slopes across each of the cracks. From these equations (2.59) and (2.60) provide the reflection and transmission coefficients R_N and T_N and equation (2.38) provides an expression for the potential everywhere in the fluid region.

In section 3 the Bloch problem for an infinite periodic array of cracks is considered and a simple algebraic condition is derived for the Bloch coefficient μ whose value governs whether

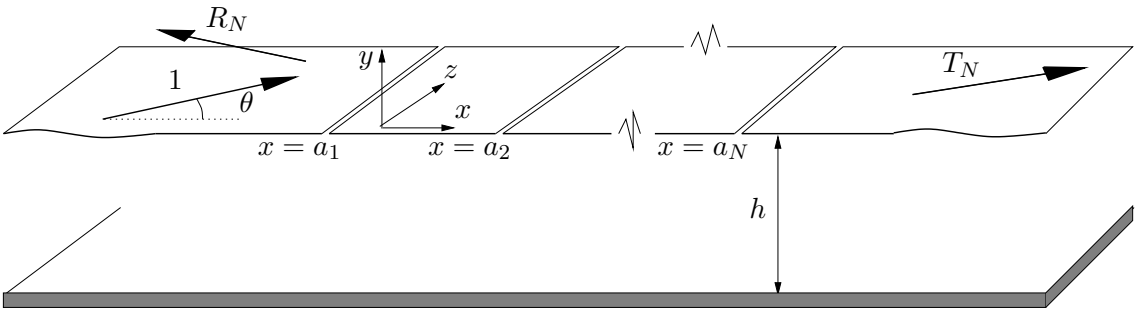

Figure 1: An illustration of the geometrical configuration of N cracks in an ice sheet on water of depth h. A wave of unit amplitude is obliquely-incident from $x = -\infty$ and gives rise to reflected and transmitted waves of complex amplitudes R_N and T_N respectively.

waves can pass through the infinite array or not. The scattering by a semi-infinite periodic array of cracks is considered in section 4 making use of the Bloch coefficient to reformulate the problem in such a way that the appropriate radiation condition is satisfied. A wide-spacing approximation to the scattering problem is developed in section 5 and is extended to consider scattering by periodic semi-infinite arrays. In doing so the intimate relationship between the scattering by finite and semi-infinite arrays of cracks and the parameter μ is highlighted.

Results from the previous sections 2, 3 and 4 are presented in section 6 and are compared with the wide-spacing approximation of section 5. In the final two sections the question of the existence of a wave motion localised to the cracks is discussed. In section 7, we address the case of two-dimensional trapped waves between two pairs of closely-spaced cracks and finally in section 8 results based on the edge wave condition are discussed for a variety of configurations.

2 Wave scattering by a finite number of cracks

2.1 Formulation of the problem

Cartesian coordinates are chosen with y directed vertically upwards. Fluid is bounded below by a flat rigid bottom on $y = -h$, $-\infty < x, z < \infty$. The ice sheet is modelled by an infinite elastic plate of small thickness, d, which floats on the surface of the fluid and has its mean position on $y = 0$. The plate is divided into $N+1$ infinite strips by N narrow parallel straight-line cracks occupying $x = a_j$, $y = 0$ for $-\infty < z < \infty$, where $a_j < a_{j+1}, j = 1, 2, \ldots, N-1$. The edges of the strips are free to move and this implies that the bending moments and the shear stresses vanish along the edges of each of the strips. In the linearisation of the equations governing the motion of the fluid and the elastic plates, it is usual to make the assumption that $d \ll 1$ so that the boundary conditions on the plates may be applied on $y = 0$. Since the entire surface of the fluid is covered by ice sheets and there is no exposed fluid surface, we may relax this condition.

In this section it is our aim to seek the reflection and transmission coefficients, denoted by R_N and T_N respectively, for an oblique wave entering the region occupied by N cracks from $x = -\infty$. The solution we construct will be used in later sections despite the fact that these sections are not all concerned with scattering of an incident wave.

Thus, we seek a velocity potential $\Phi(x, y, z, t)$ in the region $-h < y < 0$, $-\infty < x, z < \infty$

and look for a solution $\phi(x,y)$ where

$$\Phi(x,y,z,t) = \Re\{-\mathrm{i}\omega\phi(x,y)\mathrm{e}^{\mathrm{i}(lz-\omega t)}\}. \tag{2.1}$$

where ω is the radian frequency of motion and l is an assumed wavenumber in the z coordinate. The corresponding elevation of the plates is defined by $\Re\{\eta(x)\mathrm{e}^{\mathrm{i}(lz-\omega t)}\}$ where

$$\eta(x) = \left.\frac{\partial\phi}{\partial y}\right|_{y=0}, \qquad x \neq a_j,\ j = 1,2,\ldots,N. \tag{2.2}$$

It follows that the reduced velocity potential $\phi(x,y)$ satisfies

$$(\nabla^2 - l^2)\phi = 0, \quad -h < y < 0,\ -\infty < x < \infty, \tag{2.3}$$

$$\frac{\partial\phi}{\partial y} = 0, \quad y = -h,\ -\infty < x < \infty, \tag{2.4}$$

and

$$\mathcal{L}\phi \equiv \left(\beta\left(\frac{\partial^2}{\partial x^2} - l^2\right)^2 + (1-\delta)\right)\frac{\partial\phi}{\partial y} - \kappa\phi = 0, \qquad y = 0,\ x \neq a_j,\ j = 1,2,\ldots,N. \tag{2.5}$$

In the above, $\kappa = \omega^2/g$ where g is gravitational acceleration and β is defined by $\beta = D/(\rho_w g)$ where D is the flexural rigidity of the plate and ρ_w is the density of the fluid. Also $\delta = (\rho_i/\rho_w)\kappa d$ where ρ_i is the density, and d is the thickness, of the ice.

At the free edges of the plates, we must impose conditions of zero bending moments and zero shear stresses, which we express as

$$(\mathcal{B}\eta)(x) \to 0, \qquad (\mathcal{S}\eta)(x) \to 0, \qquad \text{as } x \to a_j^{\pm} \tag{2.6}$$

for $j = 1,2,\ldots,N$, where we have defined the operators $\mathcal{B}$ and $\mathcal{S}$ by

$$(\mathcal{B}u) \equiv \left(\frac{\partial^2}{\partial x^2} - \nu l^2\right)u \qquad \text{and} \qquad (\mathcal{S}u) \equiv \left(\frac{\partial^3}{\partial x^3} - \nu_1 l^2\frac{\partial}{\partial x}\right)u \tag{2.7}$$

and where $\nu_1 = 2 - \nu$ with ν Poisson's ratio.

In the course of the analysis it will be shown that quantities of particular significance associated with the edges of each of the plates are

$$P_j = \left[\eta'\right]_{x=a_j} \quad \text{and} \quad Q_j = \left[\eta\right]_{x=a_j}, \qquad j = 1,2,\ldots,N \tag{2.8}$$

where the notation $[u(x)]_{x=a} \equiv u(a^+) - u(a^-)$ will be used henceforth. Thus, in (2.8) the quantities P_j and Q_j represent the jump in the gradient and elevation (respectively) of the plates across the crack at $x = a_j$ which will, in general, be non-zero.

Apart from across each of the cracks at $x = a_j$, $\eta(x)$, $\eta'(x)$, $\eta''(x)$ and $\eta'''(x)$ are assumed to be continuous functions of x. From (2.6) this implies that $(\mathcal{B}\eta)(x)$ and $(\mathcal{S}\eta)(x)$ are continuous functions of x for $-\infty < x < \infty$. In particular we note that

$$\left[(\mathcal{B}\eta)(x)\right]_{x=a_j} = \left[(\mathcal{S}\eta)(x)\right]_{x=a_j} = 0, \qquad \text{for } j = 1,2,\ldots,N. \tag{2.9}$$

To complete the formulation of the problem, we also need to impose a radiation condition as $x \to \pm\infty$, which requires us to consider separable solutions of (2.3). Subject to the conditions (2.4) and (2.5) separable solutions of (2.3) are given by

$$\mathrm{e}^{\pm ik_n x}\, Y_n(y) \tag{2.10}$$

where $Y_n(y)$ satisfies

$$Y_n''(y) = \gamma_n^2 Y_n(y), \quad Y_n'(-h) = 0, \tag{2.11}$$

and

$$(\beta\gamma_n^4 + 1 - \delta)Y_n'(0) - \kappa Y_n(0) = 0 \tag{2.12}$$

in which we have defined

$$\gamma_n^2 = k_n^2 + l^2. \tag{2.13}$$

Equations (2.11), (2.12) and (2.13) constitute an eigensystem in which the eigenfunctions defined to be

$$Y_n(y) = \cosh\gamma_n(y+h) \tag{2.14}$$

are non-orthogonal. However it can be shown, by integrating by parts, that they do satisfy a generalised orthogonality relation, namely

$$\int_{-h}^{0} Y_n(y)Y_m(y)dy + \frac{\beta}{\kappa}(\gamma_m^2 + \gamma_n^2)Y_m'(0)Y_n'(0) = C_n\delta_{nm} \tag{2.15}$$

(see, for example, Lawrie & Abrahams 2002) where

$$C_n = \tfrac{1}{2}\{h + \kappa^{-1}(5\beta\gamma_n^4 + 1 - \delta)[Y_n'(0)/\gamma_n]^2\}. \tag{2.16}$$

Now substitution of equation (2.14) into (2.12) gives the dispersion relation

$$K(k_n) \equiv (\beta\gamma_n^4 + 1 - \delta)\gamma_n \tanh\gamma_n h - \kappa = 0 \tag{2.17}$$

governing possible values of k_n. It can be shown that this has a pair of real roots $\pm\gamma_0$ with corresponding roots $\pm k_0$ which describe progressive waves, provided $\gamma_0 > l$. Note, however, that if $\gamma_0 < l$ no such waves are possible and any motion will be confined to the cracks. Such a situation is considered later in section 8. In addition there is a sequence of pure imaginary roots $\pm k_n$ arranged so that $|k_n| < |k_{n+1}|$ for $n = 1, 2, \ldots$ and four complex roots $\pm k_{-1}$ and $\pm k_{-2}$ symmetric about the real and imaginary axes. Let the roots in the first and second quadrants be k_{-1} and k_{-2}.

Without loss of generality, a wave having wavenumber k_0 is obliquely-incident upon the array of cracks from $x = -\infty$, the crests of the waves making an angle θ with the cracks. Then $l = k_0\tan\theta = \gamma_0\sin\theta$, and we write

$$\phi(x,y) \sim \begin{cases} (\mathrm{e}^{\mathrm{i}k_0 x} + R_N\mathrm{e}^{-ik_0 x})Y_0(y), & x \to -\infty \\ T_N\mathrm{e}^{ik_0 x}Y_0(y), & x \to \infty \end{cases} \tag{2.18}$$

where R_N and T_N represent the reflection and transmission coefficients for an array of N cracks.

In order to solve the problem outlined in this section for $\phi(x,y)$ due to the scattering of waves by N cracks we shall exploit the linearity of the governing equations for $\phi(x,y)$ to express the solution in terms of a linear combination of the incident wave and certain source functions located at each of the cracks which we derive in the following section.

2.2 Derivation of source functions for a single crack

We define a pair of functions $\psi_i(x,y)$, $i=1,2$ which satisfy the following set of equations

$$(\nabla^2 - l^2)\psi_i = 0, \quad (x,y) \in D, \tag{2.19}$$

$$\frac{\partial \psi_i}{\partial y} = 0, \quad y = -h, \tag{2.20}$$

and

$$(\mathcal{L}\psi_i)(x) = 0, \qquad x \neq 0. \tag{2.21}$$

Additionally, we require that ψ_i represent outgoing waves as $|x| \to \infty$ and the source of wave energy is generated by certain jump conditions which we impose on the functions

$$w_i(x) = \left.\frac{\partial \psi_i}{\partial y}\right|_{y=0}, \qquad i = 1,2 \tag{2.22}$$

expressing the elevation of the surface, namely

$$[\mathcal{B}w_i]_{x=0} = [\mathcal{S}w_i]_{x=0} = 0, \qquad i = 1,2 \tag{2.23}$$

with

$$\left.\begin{aligned} [w_1]_{x=0} &= 0, \\ [w_1']_{x=0} &= 1, \end{aligned}\right\} \qquad \left.\begin{aligned} [w_2]_{x=0} &= 1, \\ [w_2']_{x=0} &= 0. \end{aligned}\right\} \tag{2.24}$$

As we shall see, this set of equations and conditions is sufficient to uniquely define the source functions $\psi_i(x,y)$. The reason for this particular definition is explained in the next section. In the remainder of this section we set about solving for $\psi_i(x,y)$, a process which requires taking Fourier transforms defined by

$$\overline{\psi}_i(\alpha, y) = \int_{-\infty}^{\infty} \psi_i(x,y) \mathrm{e}^{-\mathrm{i}\alpha x} dx, \tag{2.25}$$

Likewise, the transform of $w_i(x)$ is

$$\overline{w}_i(\alpha) = \left.\frac{\partial \overline{\psi_i}}{\partial y}\right|_{y=0} \tag{2.26}$$

Then $\overline{\psi}_i$ satisfies

$$\left(\frac{d^2}{dy^2} - \gamma^2\right)\overline{\psi}_i = 0, \qquad \gamma^2 = l^2 + \alpha^2 \tag{2.27}$$

and so

$$\overline{\psi}_i = A_i(\alpha)\cosh\gamma(y+h) \tag{2.28}$$

in order that the transform of the condition (2.20) on $y = -h$ be satisfied. Taking the Fourier transform of (2.21) gives

$$0 = \int_{-\infty}^{\infty} (\mathcal{L}\psi_i)(x)\mathrm{e}^{-\mathrm{i}\alpha x} dx = \Big(\beta\gamma^4 + 1 - \delta\Big)\overline{w}_i - \kappa\overline{\psi}_i|_{y=0} + \beta I_i \tag{2.29}$$

where

$$I_i(\alpha) = \int_C \left\{ g\left(\frac{d^2}{dx^2} - l^2\right)^2 w_i - w_i \left(\frac{d^2}{dx^2} - l^2\right)^2 g \right\} dx \tag{2.30}$$

and the abbrevation $g = \mathrm{e}^{-\mathrm{i}\alpha x}$ has been used. Here C is the contour $(-\infty, 0) \cup (0, \infty)$ which anticipates the effect of the discontinuities in w_i and its derivatives implied by the jump conditions (2.23), (2.24). Notice that (2.29) has been arranged so that the first term on the right-hand side of (2.29) cancels with the second part of the integral in (2.30). After integrating (2.30) by parts in two stages, it is found that

$$\begin{aligned} I_i &= \int_C \left\{ g\left(\frac{d^4}{dx^4} - 2l^2\frac{d^2}{dx^2}\right) w_i - w_i \left(\frac{d^4}{dx^4} - 2l^2\frac{d^2}{dx^2}\right) g \right\} dx \\ &= -[g(w_i''' - 2l^2 w_i')]_{x=0} + [w_i(g''' - 2l^2 g')]_{x=0} + [w_i'' g' - w_i' g'']_{x=0} \end{aligned} \tag{2.31}$$

where the contribution from $x = \pm\infty$ vanishes by assuming a small imaginary part in the frequency which will eventually be set to zero. Thus, using the fact that g and its derivatives are continuous and (2.23) to trade in higher derivatives of w_i for lower ones, we have

$$\begin{aligned} I_i &= -(\nu_1 l^2 - 2l^2) g(0)[w_i']_{x=0} + (\nu l^2 - 2l^2) g'(0)[w_i]_{x=0} - g''(0)[w_i']_{x=0} + g'''(0)[w_i]_{x=0} \\ &= -(\mathcal{B}g)(0)[w_i']_{x=0} + (\mathcal{S}g)(0)[w_i]_{x=0} \end{aligned} \tag{2.32}$$

where $\nu = 2 - \nu_1$ has been used and the definitions of $\mathcal{B}$ and $\mathcal{S}$ given by (2.7) have been reinstated. Notice that although, $(\mathcal{B}g)(0)$ and $(\mathcal{S}g)(0)$ represent simple expressions we prefer to retain the form in (2.32). Finally, imposing (2.24) for $i = 1$ and $i = 2$ gives

$$I_1 = -(\mathcal{B}g)(0), \qquad I_2 = (\mathcal{S}g)(0) \tag{2.33}$$

Having calculated I_1 and I_2 we return to (2.28) with (2.27) and find that

$$A_i(\alpha) = -\frac{\beta I_i}{K(\alpha)} \tag{2.34}$$

where

$$K(\alpha) = (\beta\gamma^4 + 1 - \delta)\gamma \sinh \gamma h - \kappa \cosh \gamma h \tag{2.35}$$

and now inverting the transform gives

$$\psi_i(x, y) = -\frac{\beta}{2\pi} \int_{-\infty}^{\infty} \frac{I_i(\alpha) \cosh \gamma(y + h)}{K(\alpha)} \mathrm{e}^{\mathrm{i}\alpha x} d\alpha \tag{2.36}$$

Alternatively, we can use the definition of I_i in terms of the operators $\mathcal{B}$, $\mathcal{S}$ to write

$$\left.\begin{aligned} \psi_1(x, y) &= \beta(\mathcal{B}\chi) \\ \psi_2(x, y) &= \beta(\mathcal{S}\chi) \end{aligned}\right\} \tag{2.37}$$

where

$$\chi(x, y) = \frac{1}{2\pi} \int_{-\infty}^{\infty} \frac{\cosh \gamma(y + h)}{K(\alpha)} \mathrm{e}^{\mathrm{i}\alpha x} d\alpha. \tag{2.38}$$

It is not difficult to show (using Fourier transform methods similar to those already described above; also see Leppington (1978)) that the function $\chi(x, y)$ satisfies

$$(\nabla^2 - l^2)\chi = 0, \qquad (x, y) \in D \tag{2.39}$$

$$\frac{\partial \chi}{\partial y} = 0, \quad y = -h, \qquad \text{with} \qquad (\mathcal{L}\chi)(x) = \delta(x), \qquad -\infty < x < \infty \tag{2.40}$$

and is outgoing as $|x| \to \infty$. That is, χ simply represents a standard Greens function for the time-harmonic point forcing at the origin on the elastic plate over water.

By deforming the contour of integration into the upper half plane for $x > 0$ and the lower half plane for $x < 0$ (noting that the small imaginary part assumed in the frequency earlier implies that the roots $\pm k_0$ have been shifted off the real line into the positive and negative half planes), $\chi(x, y)$ may be expressed in terms of an infinite series (see for example EP),

$$\chi(x, y) = \mathrm{i} \sum_{n=-2}^{\infty} \frac{Y_n'(0) Y_n(y)}{2\kappa k_n C_n} \mathrm{e}^{\mathrm{i}k_n|x|}. \tag{2.41}$$

Using (2.37) with the form of χ above gives

$$\psi_1(x, y) = -\mathrm{i}\frac{\beta}{\kappa} \sum_{n=-2}^{\infty} \frac{g_n Y_n(y)}{2k_n C_n} \mathrm{e}^{\mathrm{i}k_n|x|} \tag{2.42}$$

and

$$\psi_2(x, y) = \frac{\beta}{\kappa} \mathrm{sgn}(x) \sum_{n=-2}^{\infty} \frac{g_n' Y_n(y)}{2k_n C_n} \mathrm{e}^{\mathrm{i}k_n|x|} \tag{2.43}$$

where we have introduced the shorthand notation

$$g_n = (k_n^2 + \nu l^2) Y_n'(0) \qquad \text{and} \qquad g_n' = k_n (k_n^2 + \nu_1 l^2) Y_n'(0). \tag{2.44}$$

These are the source functions a single crack at the origin in an elastic plate on water. Finally, the far-field behaviour of $\psi_i(x, y)$, $i = 1, 2$ is given by

$$\psi_1(x, y) \sim -\mathrm{i}\frac{\beta}{\kappa} \frac{g_0}{2k_0 C_0} \mathrm{e}^{\pm \mathrm{i}k_0 x} Y_0(y), \qquad x \to \pm\infty \tag{2.45}$$

and

$$\psi_2(x, y) \sim \pm\frac{\beta}{\kappa} \frac{g_0'}{2k_0 C_0} \mathrm{e}^{\pm \mathrm{i}k_0 x} Y_0(y), \qquad x \to \pm\infty. \tag{2.46}$$

It is interesting to note that the identities

$$\frac{\beta}{\kappa} \sum_{n=-2}^{\infty} \frac{g_n' Y_n'(0)}{k_n C_n} = \frac{\beta}{\kappa} \sum_{n=-2}^{\infty} \frac{g_n Y_n'(0)}{C_n} = 1, \tag{2.47}$$

follow as a consequence of using the explicit expressions for ψ_1 and ψ_2 given in (2.42) and (2.43) in the inhomogeneous equations in (2.24). These identities were proved in the Appendix of EP (the missing factor of κ in EP is on account of the non-dimensionalisation the governing equations in that paper.)

2.3 Solution of the scattering problem

Returning to the problem for $\phi(x, y)$ of the scattering of incident waves by N cracks in the plates at $x = a_j$, $j = 1, \ldots, N$ and armed with the source functions derived in the

previous section, we can now simply state the general solution to the problem as the linear combination of the incident wave potential,

$$\phi_0(x,y) = \mathrm{e}^{\mathrm{i}k_0 x} Y_0(y), \tag{2.48}$$

and combinations of source functions, $\psi_1(x,y)$ and $\psi_2(x,y)$, located at each of the cracks, so that

$$\phi(x,y) = \phi_0(x,y) + \sum_{j=1}^{N} \Big(P_j \psi_1(x-a_j, y) + Q_j \psi_2(x-a_j, y) \Big). \tag{2.49}$$

Here, P_j and Q_j are given by (2.8), a fact that we shall soon confirm, and are as yet undetermined coefficients. The corresponding elevation of the plates is given by applying $\partial/\partial y$ to (2.49) evaluated on $y = 0$ so that

$$\eta(x) = \eta_0(x) + \sum_{j=1}^{N} \Big(P_j w_1(x-a_j) + Q_j w_2(x-a_j) \Big) \tag{2.50}$$

where $\eta_0(x) = \mathrm{e}^{\mathrm{i}k_0 x} Y_0'(0)$.

Thus, $\phi(x,y)$ clearly satisfies (2.3) and (2.4) and (2.5). Also, (2.9) is satisfied by (2.50) on account of the conditions (2.23) satisfied by $w_i(x)$, $i = 1, 2$. Consideration of the jump in $\eta(x)$ across $x = a_r$ for each $r = 1, 2, \ldots, N$ in (2.50) gives

$$\big[\eta\big]_{x=a_r} = \big[\eta_0\big]_{x=a_r} + \sum_{j=1}^{N} \Big(P_j \big[w_1(x-a_j)\big]_{x=a_r} + Q_j \big[w_2(x-a_j)\big]_{x=a_r} \Big) = Q_r \tag{2.51}$$

using (2.24) which is in accordance with the definition in (2.8). Similar consideration of the jump in $\eta'(x)$ across $x = a_r$ for $r = 1, 2, \ldots, N$ in (2.50) again using the conditions in (2.24) shows that $[\eta']_{x=a_r} = P_r$ again in accordance with the definition in (2.8).

So we have established that (2.49) satisfies all the conditions of the problem apart from the edge conditions (2.6) which we apply to (2.50) in order to determine the coefficients P_j and Q_j for $j = 1, 2, \ldots, N$. This procedure gives

$$\sum_{j=1}^{N} \big\{ P_j \big(\mathcal{B} w_1\big)(a_r - a_j) + Q_j \big(\mathcal{B} w_2\big)(a_r - a_j) \big\} = -(\mathcal{B}\eta_0)(a_r) \tag{2.52}$$

and

$$\sum_{j=1}^{N} \big\{ P_j \big(\mathcal{S} w_1\big)(a_r - a_j) + Q_j \big(\mathcal{S} w_2\big)(a_r - a_j) \big\} = -(\mathcal{S}\eta_0)(a_r) \tag{2.53}$$

for $r = 1, 2, \ldots, N$. Explicit evaluation of the various terms appearing in (2.52) and (2.53) using the definition of the operators $\mathcal{B}$ and $\mathcal{S}$, $w_i(x)$ in (2.22) in terms of $\psi_i(x,y)$ in (2.42) and (2.43), and ϕ_0 in (2.48) yields

$$\frac{\beta}{\kappa} \sum_{j=1}^{N} \big\{ Q_j s_{jr}' + \mathrm{i} P_j s_{jr} \big\} = g_0 \mathrm{e}^{\mathrm{i}k_0 a_r}, \qquad r = 1, 2, \ldots, N. \tag{2.54}$$

and

$$\frac{\beta}{\kappa} \sum_{j=1}^{N} \big\{ Q_j s_{jr}'' + \mathrm{i} P_j s_{jr}' \big\} = -g_0' \mathrm{e}^{\mathrm{i}k_0 a_r}, \qquad r = 1, 2, \ldots, N. \tag{2.55}$$

Here we have defined $d_{jr} = |a_j - a_r|$,

$$s'_{jr} = \mathrm{sgn}(j-r) \sum_{n=-2}^{\infty} \frac{g_n g'_n}{2k_n C_n} \mathrm{e}^{\mathrm{i}k_n d_{jr}}, \tag{2.56}$$

where $\mathrm{sgn}(x) = 1$, for $x \geq 0$ and $\mathrm{sgn}(x) = -1$ for $x < 0$, and

$$s_{jr} = \sum_{n=-2}^{\infty} \frac{g_n^2}{2k_n C_n} \mathrm{e}^{\mathrm{i}k_n d_{jr}}, \quad s''_{jr} = \sum_{n=-2}^{\infty} \frac{g_n'^2}{2k_n C_n} \mathrm{e}^{\mathrm{i}k_n d_{jr}}. \tag{2.57}$$

Also notice that $s'_{jj} = 0$ for $j = 1, 2, \ldots, N$ on account of the relation

$$\sum_{n=-2}^{\infty} \frac{g_n g'_n}{k_n C_n} = 0 \tag{2.58}$$

which was proved in EP.

The problem is now solved once the $2N$ linear inhomogeneous equations for the Q_j and P_j, $j = 1, 2, \ldots, N$ given by (2.54) and (2.55) are inverted. Thus, the potential $\phi(x, y)$ everywhere in the fluid domain is given by (2.49) and the corresponding plate elevation by (2.50). In particular, the reflection and transmission coefficients, R_N and T_N, can be found from (2.49) by taking the limits $x \to \pm\infty$ and using (2.18), (2.45) and (2.46) we obtain

$$R_N = -\frac{\beta}{\kappa} \sum_{j=1}^{N} \frac{\mathrm{e}^{\mathrm{i}k_0 a_j}}{2k_0 C_0} \{g'_n Q_j + \mathrm{i} g_n P_j\} \tag{2.59}$$

and

$$T_N = 1 + \frac{\beta}{\kappa} \sum_{j=1}^{N} \frac{\mathrm{e}^{-ik_0 a_j}}{2k_0 C_0} \{g'_n Q_j - \mathrm{i} g_n P_j\} \tag{2.60}$$

respectively. In the case of a single crack ($N = 1$) with $a_1 = 0$, it is straightforward to show that the expressions for the reflection and transmission coefficients are precisely those given in EP, once expressed in terms of dimensional variables.

3 The Bloch problem for an infinite periodic array of cracks

We now consider the case where there are an infinite number of cracks periodically spaced in the x-coordinate with equal separation b. In this case there is no wave incident upon the array and we are concerned with establishing whether there exist solutions that represent waves which are able to propagate through the infinite array; in this case the frequency is said to lie in a *passing band*. On the other hand, when it can be shown that waves are unable to propagate through the infinite periodic array then the frequency is said to lie in a *stopping band*. This terminology originates from solid-state physics where it is used to describe wave propagation through periodic crystal lattices (see, for example, Ashcroft & Mermin (1976)). Related work on flexural-gravity wave propagation in the presence of periodic elastic sheets on floating water has been undertaken by Chou (1998).

The Bloch problem, as is commonly referred to, for an infinite periodic array of cracks may appear to be somewhat disconnected from the main thrust of the paper up until this point due to the absence of an incident wave. However, it will be shown in the following section that the solution of the Bloch problem provides important information which is used to determine the scattering of incident waves by a semi-infinite periodically-spaced array of cracks.

Let us assume that the cracks lie on $a_j = jb$ for $-\infty < j < \infty$ so that $b = a_{j+1} - a_j$. On account of the periodicity in the geometrical configuration, we are led to making the Bloch (or Floquet) assumption that the potential across any period of width b is related by a complex constant μ expressed as

$$\phi(x-b,y) = \mu\phi(x,y), \qquad -\infty < x < \infty, \;\; -h < y < 0. \tag{3.1}$$

It follows that if $|\mu| = 1$ then $\mu = \mathrm{e}^{\mathrm{i}\alpha}$ for some $\alpha \in \mathbb{R}$ and (3.1) represents the fact that the solution simply undergoes a change in phase across each period of width b. That is, a wave is able to propagate without attenuation throughout the infinite periodic array. On the other hand, if $|\mu| \neq 1$ then (3.1) represents a solution exponentially decaying in one direction and exponentially growing in the other direction and therefore a wave cannot be supported by the infinite periodic array.

The Bloch problem is a homogeneous one in which the parameter μ plays the role of the eigenvalue. For a given angular frequency of motion, ω, we are required to find the corresponding value of μ. This is achieved most directly by manipulating the system of equations (2.54) and (2.55) already derived for the scattering problem, although alternative derivations (for example, using modified source functions for periodic cracks from the outset) are possible.

First, we notice that as a consequence of (3.1) we have

$$P_{j-1} = \mu P_j = \mu^{-j+1}P_0, \qquad \text{and} \qquad Q_{j-1} = \mu Q_j = \mu^{-j+1}Q_0. \tag{3.2}$$

These relations allow us to go directly to (2.54) and (2.55) in which the finite sum from $j = 1$ to $j = N$ is now replaced by the sum over $-\infty < j < \infty$ and the right-hand side terms in (2.54) and (2.55), which previously represented the forcing from the incident wave, are now absent so that we have

$$\left.\begin{aligned} \sum_{j=-\infty}^{\infty} \mu^{-j}\left\{Q_0 s'_{jr} + \mathrm{i}P_0 s_{jr}\right\} = 0, \\ \sum_{j=-\infty}^{\infty} \mu^{-j}\left\{Q_0 s''_{jr} + \mathrm{i}P_0 s'_{jr}\right\} = 0, \end{aligned}\right\} \qquad -\infty < r < \infty \tag{3.3}$$

Also, $d_{jr} = |a_j - a_r| = b|j-r|$ in the expressions (2.56) and (2.57) for s_{jr}, s'_{jr} and s''_{jr} which are consequently functions of $j - r$ only. This allows us to make a change of summation variable, $j' = j - r$, so that the system of equations (3.3) become (after dropping the prime on j)

$$\left.\begin{aligned} \sum_{j=-\infty}^{\infty} \mu^{-j}\left\{Q_0 \mathrm{sgn}(j) \sum_{n=-2}^{\infty} \frac{g_n g'_n \mathrm{e}^{\mathrm{i}k_n jb}}{k_n C_n} + \mathrm{i}P_0 \sum_{n=-2}^{\infty} \frac{g_n^2 \mathrm{e}^{\mathrm{i}k_n jb}}{k_n C_n}\right\} = 0, \\ \sum_{j=-\infty}^{\infty} \mu^{-j}\left\{Q_0 \sum_{n=-2}^{\infty} \frac{g_n'^2 \mathrm{e}^{\mathrm{i}k_n jb}}{k_n C_n} + \mathrm{i}P_0 \mathrm{sgn}(j) \sum_{n=-2}^{\infty} \frac{g_n g'_n \mathrm{e}^{\mathrm{i}k_n jb}}{k_n C_n}\right\} = 0, \end{aligned}\right\} \tag{3.4}$$

and the variable r is no longer present. We may interchange the order of each pair of summations and calculate the infinite sum over j explicitly. Thus, it is a straightforward algebraic exercise to show that (3.4) can be reduced to the system

$$S'Q_0 + \mathrm{i}SP_0 = 0 \tag{3.5}$$

and

$$S''Q_0 + \mathrm{i}S'P_0 = 0 \tag{3.6}$$

where

$$S' = \sum_{n=-2}^{\infty} \frac{g_n g_n'}{k_n C_n}(v_n^- + v_n^+), \quad S = \sum_{n=-2}^{\infty} \frac{g_n^2}{k_n C_n}(v_n^- - v_n^+), \quad S'' = \sum_{n=-2}^{\infty} \frac{g_n'^2}{k_n C_n}(v_n^- - v_n^+) \tag{3.7}$$

and with $v_n^{\pm}(\mu) = 1/(1-\mu \mathrm{e}^{\pm \mathrm{i}k_n b})$. That is, the Bloch eigenvalue, μ, is determined for a given ω by the satisfaction of the simple algebraic equation

$$\mathcal{D}(\mu) \equiv S'^2 - S''S = 0. \tag{3.8}$$

This equation has some important properties which we briefly discuss.

Firstly, it can be demonstrated that if μ is a Bloch eigenvalue then so is $1/\mu$. Thus, it is straightforward to show that $v_n^-(\mu) - v_n^+(\mu) = v_n^-(1/\mu) - v_n^+(1/\mu)$. Also, it can be shown that

$$v_n^-(\mu) + v_n^+(\mu) = 2 - (v_n^-(1/\mu) + v_n^+(1/\mu)) \tag{3.9}$$

so from (2.58) we see that $S'(\mu) = -S'(1/\mu)$ so that $\mathcal{D}(\mu) = \mathcal{D}(1/\mu)$. This property physically reflects the fact that waves in the the infinite periodic array have no preference in the direction in which they propagate.

Secondly, it can be shown that $\mathcal{D}(\mu)$ is real provided that μ lies either on the real axis or on the unit circle in the complex plane. In the first case, it can be shown quite straightforwardly that S', S and S'' are all real – see the discussion following equation (2.17) of the nature of the roots k_n of the dispersion relation. In the second case where $\mu = \mathrm{e}^{\mathrm{i}\alpha}$ it can be seen that $\overline{\mathcal{D}(\mu)} = \mathcal{D}(1/\mu) = \mathcal{D}(\mu)$ and hence $\mathcal{D}(\mu)$ is once again real.

4 Wave scattering by a semi-infinite periodic array of cracks

We turn our attention to a problem which is related to the two problems considered in the previous two sections, namely the scattering of waves obliquely-incident upon a *semi-infinite* periodic array of cracks. The cracks lie at $a_j = (j-1)b$ for $j = 1, 2, \ldots$ so that adjacent cracks are separated by b in accordance with the notation of section 3. The principal unknown to be determined here is R_∞, the reflection coefficient for a semi-infinite number of cracks for a wave from $x = -\infty$. The formulation and solution of section 2 for a finite number of N cracks cannot be used in its present form since the solution does not converge unformly as $N \to \infty$. This is because however large the value of N is taken, the corresponding solution represents wave scattering by a large finite array which is distinct from the truncated system of equations representing wave scattering by a semi-infinite array of cracks. The points made above are illustrated by the numerical results for large but finite arrays of cracks (see figure

6, for example), there is an increasingly complicated response in the reflection coefficient due to multiple interference effects between the ends of the array of cracks.

The crucial distinction between a large finite array of cracks and a semi-infinite array of cracks is in the assumed form of the potential at $x \to \infty$. Thus, for a semi-infinite array, we make the assertion that far enough into the array of cracks the wave field starts to respond as though it is part of an infinite array. Similar ideas have been used by Nishimoto & Ikuno (1999) who considered the scattering of electromagnetic waves by a semi-infinite periodic diffraction grating.

Referring to the Bloch modes for an infinite array, we expect $P_{j-1} \sim \mu P_j$ and $Q_{j-1} \sim \mu Q_j$ as $j \to \infty$, where μ is the appropriate Bloch eigenvalue for the corresponding infinite periodic array at the particular frequency being considered which we assume has be found from (3.8). Hence, we introduce new coefficients

$$\widehat{P}_j = P_{j-1} - \mu P_j \qquad \text{and} \qquad \widehat{Q}_j = Q_{j-1} - \mu Q_j \tag{4.1}$$

for $j = 2, 3, \ldots$ all of which, by assumption, will tend to zero as $j \to \infty$.

Our aim is to reformulate this semi-infinite scattering problem in terms of $\widehat{P}_j$ and $\widehat{Q}_j$ coefficients so as to obtain a convergent infinite system of equations. To achieve this we go directly to (2.54) and (2.55) with $N = \infty$. Thus, we first note from (2.56) and (2.57) that for $r \geq 2$, $s_{j-1,r-1} = s_{jr}$, $s'_{j-1,r-1} = s'_{jr}$ and $s''_{j-1,r-1} = s''_{jr}$ so that we may write (2.54) as

$$\frac{\beta}{\kappa} \sum_{j=2}^{\infty} \left\{ Q_{j-1} s'_{jr} + \mathrm{i} P_{j-1} s_{jr} \right\} = g_0 \mathrm{e}^{\mathrm{i}k_0 a_{r-1}}, \qquad r = 2, 3, \ldots \tag{4.2}$$

and (2.55) as

$$\frac{\beta}{\kappa} \sum_{j=2}^{\infty} \left\{ Q_{j-1} s''_{jr} + \mathrm{i} P_{j-1} s'_{jr} \right\} = -g'_0 \mathrm{e}^{\mathrm{i}k_0 a_{r-1}}, \qquad r = 2, 3, \ldots \tag{4.3}$$

By subtracting μ times (2.54) from (4.2) and using (4.1) we have

$$\frac{\beta}{\kappa} \sum_{j=2}^{\infty} \left\{ \widehat{Q}_j s'_{jr} + \mathrm{i} \widehat{P}_j s_{jr} \right\} - \mu \frac{\beta}{\kappa} \left(Q_1 s'_{1,r} + \mathrm{i} P_1 s_{1,r} \right) = g_0 \mathrm{e}^{\mathrm{i}k_0 a_r} (\mathrm{e}^{-\mathrm{i}k_0 b} - \mu) \tag{4.4}$$

for $r = 2, 3, \ldots$. Similarly, subtracting μ times (2.55) from (4.3) we results in

$$\frac{\beta}{\kappa} \sum_{j=2}^{\infty} \left\{ \widehat{Q}_j s''_{jr} + \mathrm{i} \widehat{P}_j s'_{jr} \right\} - \mu \frac{\beta}{\kappa} \left(Q_1 s''_{1,r} + \mathrm{i} P_1 s'_{1,r} \right) = -g'_0 \mathrm{e}^{\mathrm{i}k_0 a_r} (\mathrm{e}^{-\mathrm{i}k_0 b} - \mu) \tag{4.5}$$

for $r = 2, 3, \ldots$. We need to supplement (4.4) and (4.5) with corresponding equations for $r = 1$. Hence, from (2.54) with $r = 1$ we have

$$\frac{\beta}{\kappa} \sum_{j=1}^{\infty} \left\{ Q_j s'_{j,1} + \mathrm{i} P_j s_{j,1} \right\} = g_0 \mathrm{e}^{\mathrm{i}k_0 a_1}. \tag{4.6}$$

To be of any use, (4.6) needs to be expressed in terms of the unknowns already occurring in (4.4) and (4.5). First we solve (4.1) as a recurrence relation for P_j, Q_j, $j = 2, 3, \ldots$ in terms of $\widehat{P}_j$, $\widehat{Q}_j$, P_1 and Q_1, so that

$$P_j = \frac{1}{\mu^{j-1}} P_1 - \sum_{k=2}^{j} \frac{1}{\mu^{j+1-k}} \widehat{P}_k, \qquad Q_j = \frac{1}{\mu^{j-1}} Q_1 - \sum_{k=2}^{j} \frac{1}{\mu^{j+1-k}} \widehat{Q}_k. \tag{4.7}$$

Substituting into (4.6), gathering together the terms associated with the various coefficients, and making some elementary manipulations, gives

$$\frac{\beta}{\kappa}\left[Q_1\sum_{k=1}^{\infty}\frac{s'_{k,1}}{\mu^{k-1}}+\mathrm{i}P_1\sum_{k=1}^{\infty}\frac{s_{k,1}}{\mu^{k-1}}\right]-\frac{\beta}{\kappa}\sum_{j=2}^{\infty}\left\{\widehat{Q}_j\sum_{k=j}^{\infty}\frac{s'_{k,1}}{\mu^{k+1-j}}+\mathrm{i}\widehat{P}_j\sum_{k=j}^{\infty}\frac{s_{k,1}}{\mu^{k+1-j}}\right\}=g_0\mathrm{e}^{\mathrm{i}k_0a_1} \quad (4.8)$$

By defining new coefficients

$$t'_j=-\sum_{k=j}^{\infty}\frac{s'_{k,1}}{\mu^{k+1-j}},\qquad t_j=-\sum_{k=j}^{\infty}\frac{s_{k,1}}{\mu^{k+1-j}}, \quad (4.9)$$

we may write (4.8) more simply as

$$\frac{\beta}{\kappa}\sum_{j=2}^{\infty}\left\{\widehat{Q}_jt'_j+\mathrm{i}\widehat{P}_jt_j\right\}-\mu\frac{\beta}{\kappa}\big(Q_1t'_1+\mathrm{i}P_1t_1\big)=g_0\mathrm{e}^{\mathrm{i}k_0a_1} \quad (4.10)$$

which has been transformed into the desired set of unknown coefficients. Using the definitions for $s'_{k,1}$ and $s_{k,1}$ from (2.56) and (2.57), noting that $d_{k,1}=(k-1)b$, it is readily shown that the summation over k defining t'_j and t_j in (4.9) can be performed explicitly, resulting in the simplified expressions

$$t'_j=\sum_{n=-2}^{\infty}\frac{g_ng'_n}{2k_nC_n}\frac{\mathrm{e}^{\mathrm{i}k_nd_{j,1}}}{(\mathrm{e}^{\mathrm{i}k_nb}-\mu)},\qquad j=1,2,\ldots \quad (4.11)$$

and

$$t_j=\sum_{n=-2}^{\infty}\frac{g_n^2}{2k_nC_n}\frac{\mathrm{e}^{\mathrm{i}k_nd_{j,1}}}{(\mathrm{e}^{\mathrm{i}k_nb}-\mu)},\qquad j=1,2,\ldots \quad (4.12)$$

We can employ a similar procedure to the last equation to be considered, which is (2.55) with $r=1$. Thus, we find that

$$\frac{\beta}{\kappa}\sum_{j=2}^{\infty}\left\{\widehat{Q}_jt''_j+\mathrm{i}\widehat{P}_jt'_j\right\}-\mu\frac{\beta}{\kappa}\big(Q_1t''_1+\mathrm{i}P_1t'_1\big)=-g'_0\mathrm{e}^{\mathrm{i}k_0a_1} \quad (4.13)$$

where we have defined

$$t''_j=\sum_{n=-2}^{\infty}\frac{g'^2_n}{2k_nC_n}\frac{\mathrm{e}^{\mathrm{i}k_nd_{j,1}}}{(\mathrm{e}^{\mathrm{i}k_nb}-\mu)},\qquad j=1,2,\ldots \quad (4.14)$$

To summarise, the solution of the problem for the semi-infinite scattering of waves is embodied in the solution of the infinite system of equations (4.4), (4.5) for $r=2,3,\ldots$ supplemented by (4.10) and (4.13) which are posed in terms of the unknown coefficients Q_1, P_1 and $\widehat{Q}_j$, $\widehat{P}_j$ for $j=2,3,\ldots$. By construction, the hatted coefficients will tend to zero as j increases and thus we anticipate a truncation of the infinite system of equations to converge as the truncation size is increased.

Finally, we need to determine the reflection coefficient R_∞. Thus, from (2.59) with $N=\infty$

$$R_\infty=-\frac{\beta}{\kappa}\sum_{j=1}^{\infty}\frac{\mathrm{e}^{\mathrm{i}k_0a_j}}{2k_0C_0}\big(g'_0Q_j+\mathrm{i}g_0P_j\big) \quad (4.15)$$

and we mimic earlier manipulations by writing to express the system in terms of the desired coefficients and eventually find that

$$R_\infty = \frac{\beta}{2k_0C_0\kappa}\left[\mu u_1\big(g_0'Q_1 + \mathrm{i}g_0P_1\big) - \sum_{j=2}^{\infty} u_j\big(g_0'\widehat{Q}_j + \mathrm{i}g_0\widehat{P}_j\big)\right] \tag{4.16}$$

where

$$u_j = \mathrm{e}^{\mathrm{i}k_0d_{j,1}}/(\mathrm{e}^{\mathrm{i}k_0b} - \mu), \qquad j = 1, 2, \ldots \tag{4.17}$$

It is noteworthy that the formulation derived in this section relies upon the introduction of the arbitrary parameters t_1, t_1', t_1'' and u_1 each of which has been chosen to give maximum simplification in the final expressions. Despite this, when different values for these parameters are used the numerical results are not affected.

5 The wide-spacing approximation for periodic arrays of cracks

The wide-spacing approximation (see, for example, Newman (1965)) may be applied to the case of a finite number of cracks with arbitrary spacing between them. Thus approximations to the reflection and transmission coefficients may be derived on the basis that the spacing between adjacent cracks is sufficiently large with respect to the length of propagating waves to assume that the effect of evanescent wave interactions between adjacent cracks is negligible. The interaction of waves at any one crack in the array is characterised by the two incoming and the two outgoing propagating wave amplitudes and by the (assumed known) reflection and transmission coefficients for a single crack in isolation and located at the origin. It is usual to proceed by expressing this interaction in terms of either a 2×2 scattering matrix or a 2×2 transition matrix from which elementary linear algebra can be used to derive the reflection and transmission coefficients R_N and T_N for the entire array. The expressions for R_N and T_N for arbitrary crack spacing are not particularly attractive as they are in terms of the products of N transition matrices.

We shall not consider using the wide-spacing approximation for arbitrary arrangement of cracks. Instead we shall take advantage of the fact that simple formulae for R_N and T_N have previously been developed in the particularly interesting case where the array has periodicity (either of finite or semi-infinite extent). The reader is referred to the work of Kriegsmann (2003) which covers both cases mentioned above, although we shall adopt the more succint notation of Chamberlain & Porter (1995) who had previously developed the wide-spacing result for finite periodic arrays.

Firstly, for a periodic array of N cracks located at $a_j = (j-1)b$, $j = 1, 2, \ldots, N$ it is possible to show using the methods of Kriegsmann (2003) or Chamberlain & Porter (1995) that

$$R_N = \frac{R_1\sigma_N}{\sigma_N - \lambda T_1\sigma_{N-1}} \qquad \text{and} \qquad T_N = \frac{T_1}{\lambda^{N-1}(\sigma_N - \lambda T_1\sigma_{N-1})}, \tag{5.1}$$

where $\lambda = \mathrm{e}^{\mathrm{i}k_0b}$, R_1 and T_1 are the reflection and transmission coefficients for a single crack at $x = 0$ for a wave incident from $x = -\infty$, and

$$\sigma_N = \sin(N\alpha)/\sin\alpha \tag{5.2}$$

where α is defined by

$$\cos\alpha = \tau = \frac{\cos(\arg(T_1) + k_0 b)}{|T_1|}. \tag{5.3}$$

Different cases arise depending upon the value of τ in (5.3) above which has been presented in anticipation of the case where $|\tau| < 1$. In this case, $\alpha \in [0, \pi]$ provided $\sin(\arg(T_1)+k_0 b) > 0$, whilst $\alpha \in [\pi, 2\pi]$ for $\sin(\arg(T_1) + k_0 b) < 0$. Other cases that arise are when (i) $\tau = \pm 1$ where σ_N in (5.2) is replaced by $(\pm 1)^{(N+1)}N$; (ii) $\tau > 1$, where we replace α by $\mathrm{i}\alpha'$ so that $\sigma_N = \sinh N\alpha'/\sinh\alpha'$ and (iii) $\tau < -1$ where we let $\alpha = \pi + \mathrm{i}\alpha'$ so that $\sigma_N = (-1)^{N+1}\sinh N\alpha'/\sinh\alpha'$.

From (5.1) it is also possible to show that

$$|R_N|^2 = \frac{|R_1|^2\sigma_N^2}{|R_1|^2\sigma_N^2 + |T_1|^2}, \qquad \text{and} \qquad |T_N|^2 = \frac{|T_1|^2}{|R_1|^2\sigma_N^2 + |T_1|^2}. \tag{5.4}$$

An expression for R_∞, which we define as the reflection coefficient for a semi-infinite periodic array of cracks, cannot be found directly from (5.1) by taking the limit as $N \to \infty$ on account of the increasingly oscillatory behaviour of σ_N. However, this difficulty can be overcome by introducing a small amount of artificial dissipation into the scattering process before taking the limit $N \to \infty$ and subsequently letting the dissipation tend to zero. This procedure, which is widely used in conjunction with the Weiner-Hopf technique, has been implemented by Kryiazidou *et al* (2000) and Botten *et al* (2001) in related problems. It has evidently also been used by Kriegsmann (2003) in deriving his expression for R_∞ which is equivalent to (5.5) below, although Kriegsmann makes no reference to this in his paper.

Thus we replace α by $\alpha + \mathrm{i}\varepsilon$ where $0 < \varepsilon \ll 1$ represents a small dissipative effect which ensures, via the particular definition of α, that $|T_N| \to 0$ as $N \to \infty$ in all cases. It follows that $\sigma_{N-1}/\sigma_N \to \mathrm{e}^{\mathrm{i}\alpha}\mathrm{e}^{-\varepsilon}$ after taking the limit $N \to \infty$. Finally, letting $\varepsilon \to 0$ results in

$$R_\infty = \frac{R_1}{1 - \lambda\mu T_1} \tag{5.5}$$

where $\mu = \mathrm{e}^{\mathrm{i}\alpha}$. This expression holds for $|\tau| < 1$ whilst for $\tau \geq 1$, $\mu = \mathrm{e}^{-\alpha'}$ and for $\tau \leq -1$, $\mu = -\mathrm{e}^{-\alpha'}$.

It is important to note that the particular μ used in (5.5) is just one of the roots of the quadratic equation

$$\mu^2 - 2\tau\mu + 1 = 0 \tag{5.6}$$

which is fundamental to the derivation of the expressions for R_N and T_N presented in (5.1). It is of no coincidence that μ is used both in (5.6) and earlier in (3.1) since the values of μ determined by (5.6) are precisely the eigenvalues of the Bloch problem (albeit under wide-spacing assumptions) which then determine the nature of wave propagation through an infinite periodic array.

When $|\tau| > 1$, it can be shown directly from (5.5) that $|R_\infty| = 1$ and corresponds to a stopping band in the infinite periodic array. In this case, it can easily be seen from (5.4) that $|R_N| \to 1$ and $|T_N| \to 0$ as $N \to \infty$ in the finite periodic array as we might expect.

For $|\tau| < 1$ it can be shown that $|R_\infty| < 1$ and in this case energy is transmitted through the semi-infinite periodic array corresponding to the presence of a passing band in the infinite array. In this case $|R_N|$ and $|T_N|$ in the finite array have a complicated behaviour as k_0 varies on account of the oscillatory nature of σ_N. Using (5.4) we note that values of wavenumber k_0

at which $R_N = 0$ are given by $\sin N\alpha = 0$. Furthermore, as noted by Porter & Porter (2003) (also see Botten *et al* 2001), $|T_N|^2$ is bounded below by $|T_1|^2 \sin^2\alpha/(|T_1|^2 \sin^2\alpha + |R_1|^2)$ and this allows us to derive an envelope function $R_b(k_0)$ independent of N which bounds $|R_N|$ from above such that

$$|R_N| \leq R_b = \frac{|R_1|}{|\sin(\arg(T_1) + k_0 b)|}, \qquad \text{for all } N. \tag{5.7}$$

This bound applies only in $|\tau| \leq 1$ and is such that $R_b = 1$ when $|\tau| = 1$.

6 Results for wave scattering

In this section we present a set of results concerned with the scattering of an incident wave by a range of crack configurations. In particular we shall combine, for large periodic arrays of cracks the results from sections 2, 3, and 4 to show the close connection between wave scattering by large finite arrays, semi-infinite arrays and wave propagation in infinite periodic arrays. In each case, results can be compared with the analogeous results which are obtained using the wide-spacing approximation of section 5.

Since this study is motivated by flexural wave propagation in ice sheets, we adopt the parameters for ice used in Fox & Squire (1994). Thus the flexural rigidity, D is defined by $D = Ed^3/(12(1-\nu^2))$ where E is Young's modulus and d is the thickness of the ice. We use values of $E = 5$GPa, $\nu = 0.3$, $\rho_w = 1025\text{kgm}^{-3}$ and $\rho_i = 925\text{kgm}^{-3}$ which defines $\beta = 45536d^3$ and $\delta = \delta'\kappa d$ where $\delta' = \rho_i/\rho_w = 0.9$ and where $\kappa = \omega^2/g$. We also introduce the non-dimensional quantity $\beta' = \beta/d^4 = 45536/d$.

To illustrate the main features of our results, we shall fix $d = 1$m as the ice thickness, although the results are qualitatively similar for other values of d. For similar reasons, we shall fix the depth of the water by choosing $h/d = 40$ so that apart from at very long wavelengths the results approximate results for an infinite depth fluid. We shall also assume wave incidence normal to the cracks so that $\theta = 0$ and hence $l = 0$. For shallower depths and oblique wave incidence the results have been shown to exhibit similar features to those we have chosen to present and the reader is referred to EP where these parameters were varied for wave scattering by a single crack.

We choose to measure variation in reflection and transmission coefficients against the non-dimensional wavenumber of the incident waves, $\gamma_0 d$ (equivalent to $k_0 d$ for normal incidence) in most cases although we shall also use the wavelength to ice sheet thickness ratio λ_0/d where $\lambda_0 = 2\pi/\gamma_0$.

For a detailed outline of the numerical procedure employed, the reader is referred to EP. The values of the infinite sums required in, for example, the calculation of (2.54) and (2.55) are obtained by truncation to 1000 terms, which gives an accuracy in excess of 6 decimal places in all cases considered. In all computations the energy relation $|R_N|^2 + |T_N|^2 = 1$ was satisfied to within machine accuracy.

First, let us consider scattering by a pair of cracks. In figure 2 we show the variation of $|T_2|$ with λ_0/d for a pair of cracks separated by $b/d = 20$ computed from the exact theory (see equations (2.54) and (2.55)). Also shown in figure 2 using the dashed curve are the corresponding results using the wide-spacing approximation (computed using equation (5.4)) which is in good agreement for $\lambda_0/d \lesssim 30$. It is not surprising that the wide-spacing approximation is not so good for larger values of λ_0, since it is based on the assumption that

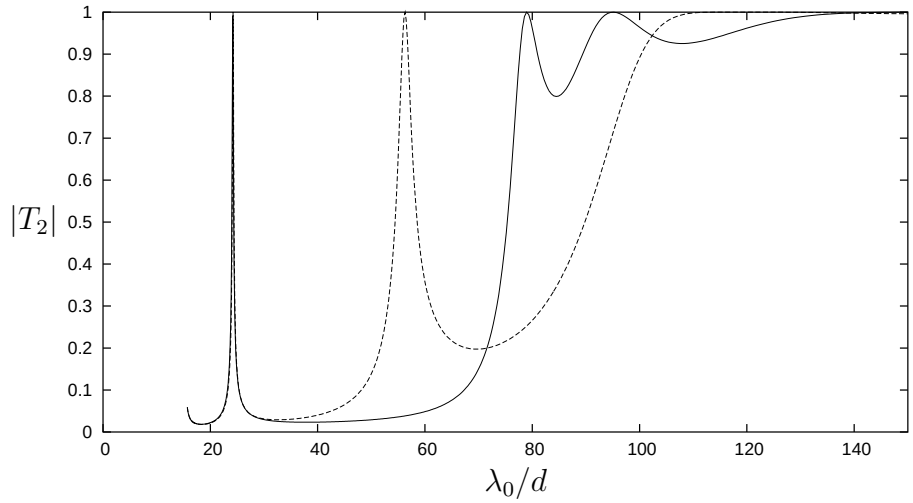

Figure 2: The modulus of transmission coefficient against non-dimensional wavelength λ_0/d for $N = 2$ cracks separated by $b/d = 20$. Also shown (dashed curve) is the corresponding curve using the wide-spacing approximation.

the wavelength is 'small' in comparison with the spacing. Notice the occurrence of zeros of reflection predicted by the exact theory, a common feature in wave scattering by multiple bodies.

In figure 3 we show $|T_2|$ against k_0d for $b/d = 40$, double the spacing in figure 2. Again, the wide-spacing approximation is included and performs well for values of $k_0d \gtrsim 0.12$ (which translates to $\lambda_0/d \lesssim 50$) suggesting a general rule that the wide-spacing approximation is valid for $\lambda_0 \lesssim b$. In figure 3 values of $k_0d > 0.1$ where $|T_2| = 1$ appear periodically and this can be explained by examination of the wide-spacing formulae (5.1)–(5.3) where $R_2 = 0$ whenever $\sigma_2 = 0$.

A more interesting effect occurs when the spacing between a pair of cracks is reduced, as illustrated in figure 4 where $b/d = 0.5$ has been used. For this narrow crack separation, there is little merit in making a comparison with the wide spacing approximation. We have instead included a separate curve (dashed) which shows the modulus of the transmission coefficient for a *single* crack, which we might expect to approximate the transmission coefficient for two closely-spaced cracks. This is indeed the case for $k_0d \lesssim 0.08$ and to a lesser extent for $k_0d > 0.12$. However, the curve of $|T_2|$ exhibits a strange behaviour for $0.1 < k_0d < 0.12$ ($50 \lesssim \lambda_0/d \lesssim 60$). In this interval we note the occurrence of two zeros of transmission (at $k_0d \approx 0.11255$ and $k_0d \approx 0.11628$), and two zeros of reflection (at $k_0d \approx 0.1066$ and $k_0d \approx 0.11613$). Of course, we have already observed zeros of reflection in figures 2 and 3 for much larger crack spacings. In contrast, the zeros of transmission only occur for a crack separation of $b/d \lesssim 1$. This feature is illustrated more clearly in figure 5, showing the variation of wavenumber k_0d at which zeros of R_2 and T_2 occur with spacing, b/d. This figure has some similarities with McIver (1985), enhanced in Porter & Evans (1995), who were concerned with locating zeros of reflection and transmission by two surface-piercing rigid vertical barriers in water of finite depth. Figure 5 also shows the behaviour of the zeros of reflection and transmission as b/d tends to zero. The sharp spike in $|T_2|$ in figure 4 is due to the fact that the upper two curves in figure 5 are close together at $b/d = 0.5$ and they continue to get closer together as b/d is reduced further. The less pronounced jump from

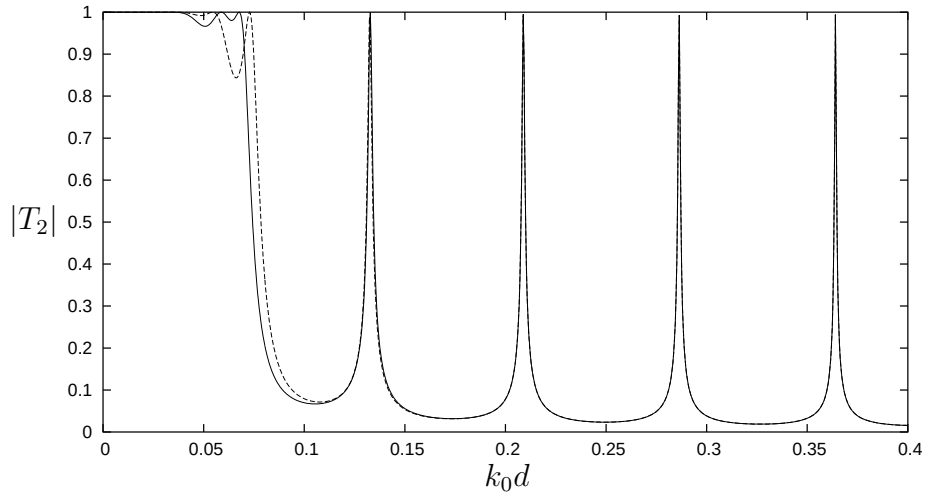

Figure 3: The modulus of transmission coefficient against non-dimensional wavenumber k_0d for $N = 2$ cracks separated by $b/d = 40$. Also shown (dashed curve) is the corresponding curve using the wide-spacing approximation.

$R_2 = 0$ to $T_2 = 0$ in figure 4 also narrows as $b/d \to 0$, although much more slowly. It is found that the curve of $|T_2|$ does tend to the curve for a single crack as $b/d \to 0$ apart from close to the zeros of R_2 and T_2 predicted by figure 5.

We can go some way to describing the singular behaviour for a pair of cracks in the limit as $b/d \to 0$. It is believed that a complete description may require some careful asymptotic analysis, beyond the scope of this paper.

We are able to express equations (2.54) and (2.55) in the form

$$\left.\begin{aligned} \mathbf{S}'\mathbf{q} + \mathbf{S}\mathbf{p} &= \mathbf{g} \\ \mathbf{S}''\mathbf{q} + \mathbf{S}'\mathbf{p} &= \mathbf{g}' \end{aligned}\right\} \tag{6.1}$$

where $\{\mathbf{S}'\}_{rj} = s'_{rj}$ etc..., and $\{\mathbf{q}\}_j = Q_j$, $\{\mathbf{p}\}_j = iP_j$ whilst $\{\mathbf{g}\}_j = \kappa g_0 \mathrm{e}^{\mathrm{i}ka_j}/\beta$ and $\{\mathbf{g}'\}_j = -\kappa g'_0 \mathrm{e}^{\mathrm{i}ka_j}/\beta$.

The particular form of the solution in (6.1) allows us to analyse the behaviour of the solution in the case of $N = 2$ cracks separated by a distance b, say, in the limit as $b \to 0$. Hence, supposing that $a_1 = 0$ and $a_2 = b$, we find that, as $b \to 0$ and ignoring $O(b^2)$ terms,

$$\mathbf{S}' \to \begin{pmatrix} s' & -s' - b\tilde{s}' \\ s' + b\tilde{s}' & s' \end{pmatrix}, \quad \mathbf{S} \to \begin{pmatrix} s & s + b\tilde{s} \\ s + b\tilde{s} & s \end{pmatrix}, \quad \mathbf{S}'' \to \begin{pmatrix} s'' & s'' + b\tilde{s}'' \\ s'' + b\tilde{s}'' & s'' \end{pmatrix} \tag{6.2}$$

where

$$s' = \sum_{n=-2}^{\infty} \frac{g_n g'_n}{2k_n C_n} = 0, \qquad s = \sum_{n=-2}^{\infty} \frac{g_n^2}{2k_n C_n}, \qquad s'' = \sum_{n=-2}^{\infty} \frac{g_n'^2}{2k_n C_n}, \tag{6.3}$$

using the identity (2.58) to simplify the first sum, and

$$\tilde{s}' = i \sum_{n=-2}^{\infty} \frac{g_n g'_n}{2C_n}, \quad \tilde{s} = i \sum_{n=-2}^{\infty} \frac{g_n^2}{2C_n}, \quad \tilde{s}'' = i \sum_{n=-2}^{\infty} \frac{g_n'^2}{2C_n}.$$

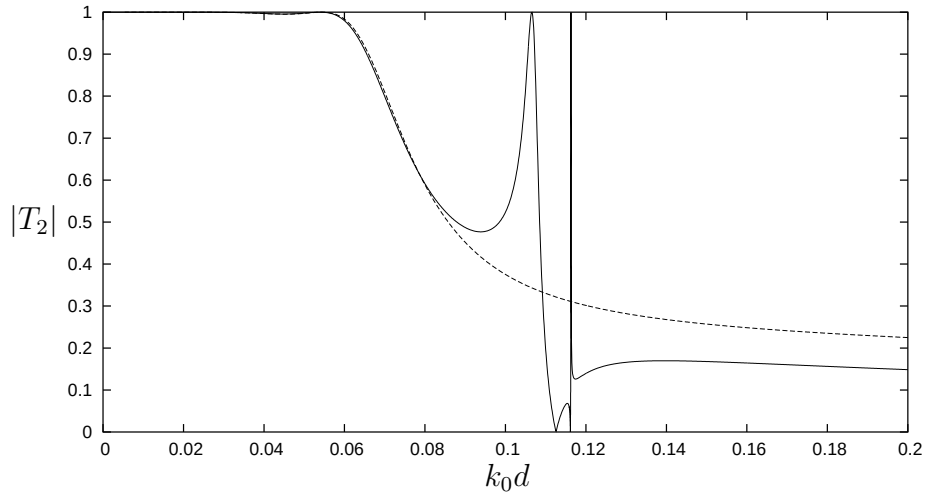

Figure 4: The modulus of transmission coefficient against non-dimensional wavenumber $k_0 d$ for $N = 2$ cracks separated by $b/d = 0.5$. Also shown (dashed curve) is $|T_1|$ for a single crack.

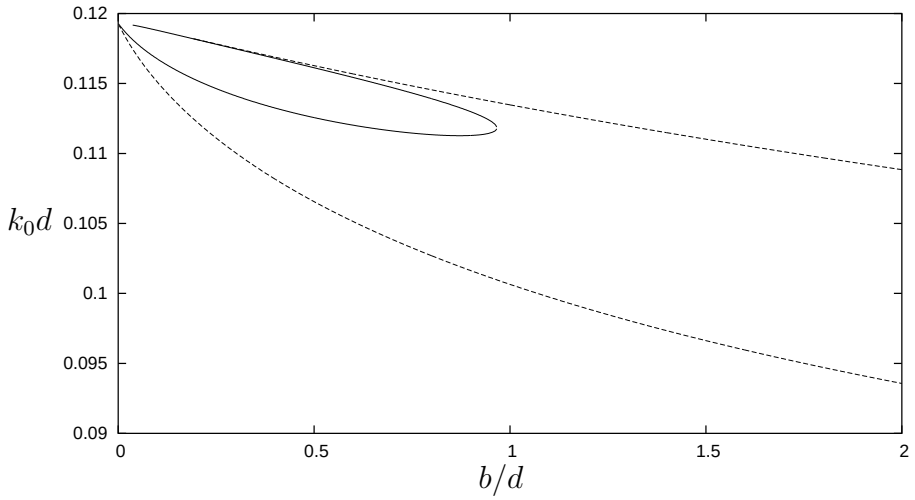

Figure 5: Curves showing the variation of $k_0 d$ at which zeros of T_2 (solid) and R_2 (dashed) occur as the spacing, b/d, between $N = 2$ cracks is varied.

It is easily seen from (6.1) and (6.2) that the solution vectors $\mathbf{p}$ and $\mathbf{q}$ are singular in the limit as $b \to 0$. In fact we find from (6.1) after discarding $O(b)$ terms that

$$\left.\begin{aligned} is(P_1 + P_2) &= \kappa g_0/\beta, \\ s''(Q_1 + Q_2) &= -\kappa g_0'/\beta, \end{aligned}\right\} \qquad \text{as } b \to 0. \tag{6.4}$$

By scaling the coordinates in the governing equations by a factor b so that the cracks now lie at $x' = 0$ and $x' = 1$, and taking the limit as $b \to 0$, it can be shown that the plate now occupying $0 < x' < 1$ has an elevation of $\phi_{y'}(x', 0) = Ax' + B$ for some constants A and B. That is, a small plate is approximately rigid with two modes of motion. Returning to the original coordinates, this implies that $\eta(0^+) \to \eta(b^-)$ and $\eta'(0^+) \to \eta'(b^-)$ From the definition of P_j in (2.8) we surmise that $P_1 + P_2 \to \eta'(b^+) - \eta'(0^-)$ as $b \to 0$ which is just

the jump in the slope of the edges of the two *semi-infinite* plates occupying $x > b$ to $x < 0$. In a similar manner we argue that $Q_1 + Q_2 \to \eta(b^+) - \eta(0^-)$ as $b \to 0$. With this limiting form, it turns out that (6.4) coincides with the results of EP for an ice sheet containing a *single* crack. Thus, although the system of equations for two cracks become singular as the spacing is reduced to zero, there is a sense in which it does exist limiting behaviour helping to explain the spikey behaviour observed in figure 4.

A more careful analysis using equation (6.1) and (6.2) whilst retaining terms of $O(b)$ allows us to show that $\mathbf{p}$ and $\mathbf{q}$ behave like $O(1/b^2)$ as $b \to 0$.

An alternative approach is to express the problem as the sum of symmetric and anti-symmetric components. Then numerically, it can be shown that associated with the sharper spike in figure 4 is a large antisymmetric response in the plate occupying $0 < x < b$ whilst the less pronounced jump in the transmission coefficient for the lower value of $k_0 d$ is associated with a symmetric excitation in the plate.

We now move on to look at larger periodic arrays of cracks and illustrate the main features with a periodicity of $b/d = 20$. In figure 6(a) and (b) we plot the modulus of reflection coefficient against $k_0 d$ for $N = 4$ and $N = 8$ cracks respectively based on the exact system of equations in (2.54) and (2.55). The curves of $|R_4|$ and $|R_8|$ exhibit oscillatory behaviour for certain intervals of $k_0 d$ and are very close to $|R_N| = 1$ in others. In the oscillatory intervals, the reflection coefficient should touch zero although the resolution of the numerical results has not picked out this feature. Overlaid on each of the curves in figures 6(a) and (b) is a bold curve showing $|R_\infty|$, the reflection coefficient for a semi-infinite periodic array of cracks. This has been computed from (4.16) and has used the appropriate value of μ found from solving (3.8) for the Bloch problem. In the computation of R_∞, we are required to truncate an infinite system of equations for coefficients $\widehat{P}_j$ and $\widehat{Q}_j$, $j = 2, 3, \ldots$ which are defined to tend to zero as $j \to \infty$. It was found numerically that truncating to 16 terms was sufficient to obtain in excess of four decimal places accuracy in R_∞.

In order to illustrate how instrumental the value of μ is, we add figure 6(c) below figures 6(a) and 6(b) showing the variation of $\arg(\mu) \in [0, \pi]$ when μ is on the unit circle in the complex plane (solid curve) and $|\mu| \leq 1$ when μ is on the real line (dashed curve). It can clearly be seen that when μ is real, corresponding to a stopping band in the infinite array, $|R_\infty| = 1$ as we expect. Also, for a finite array of N cracks, $|R_N| \to 1$, although this limit is approach much more slowly for the first stopping band ($k_0 d \approx 0.07$) than in later stopping bands. This can be explained by the relative departure of $|\mu|$ from unity in each of the stopping bands; the smaller the value of $|\mu|$, the greater the decay through the array.

In contrast, when μ lies on the unit circle in the complex plane, $|R_\infty| < 1$ as required and the corresponding behaviour of $|R_N|$ for $N = 4$ and $N = 8$ is oscillatory.

We have shown that if μ is a Bloch eigenvalue then so is $1/\mu$ which implies that eigenvalues on the complex unit circle occur as complex conjugates and for real eigenvalues as reciprocals. When performing the computation for R_∞, derived in section 4, and which involves the Bloch eigenvalue μ, we must ensure that we use the appropriate eigenvalue.

In the case where μ is real, the choice is obvious; we choose the value of μ whose modulus is less than unity. This ensures, through the definition of $\widehat{P}_j$, $\widehat{Q}_j$ in (4.1) that the wave field decays as $x \to \infty$ and so the solution is bounded.

The situation is less clear in the case where μ lies on the complex unit circle. When an expression for R_∞ was derived in section 5 using the wide-spacing approximation, we were able to select the appropriate eigenvalue by using arguments involving dissipation. This was only made possible on account of the explicit nature of the solution that was found

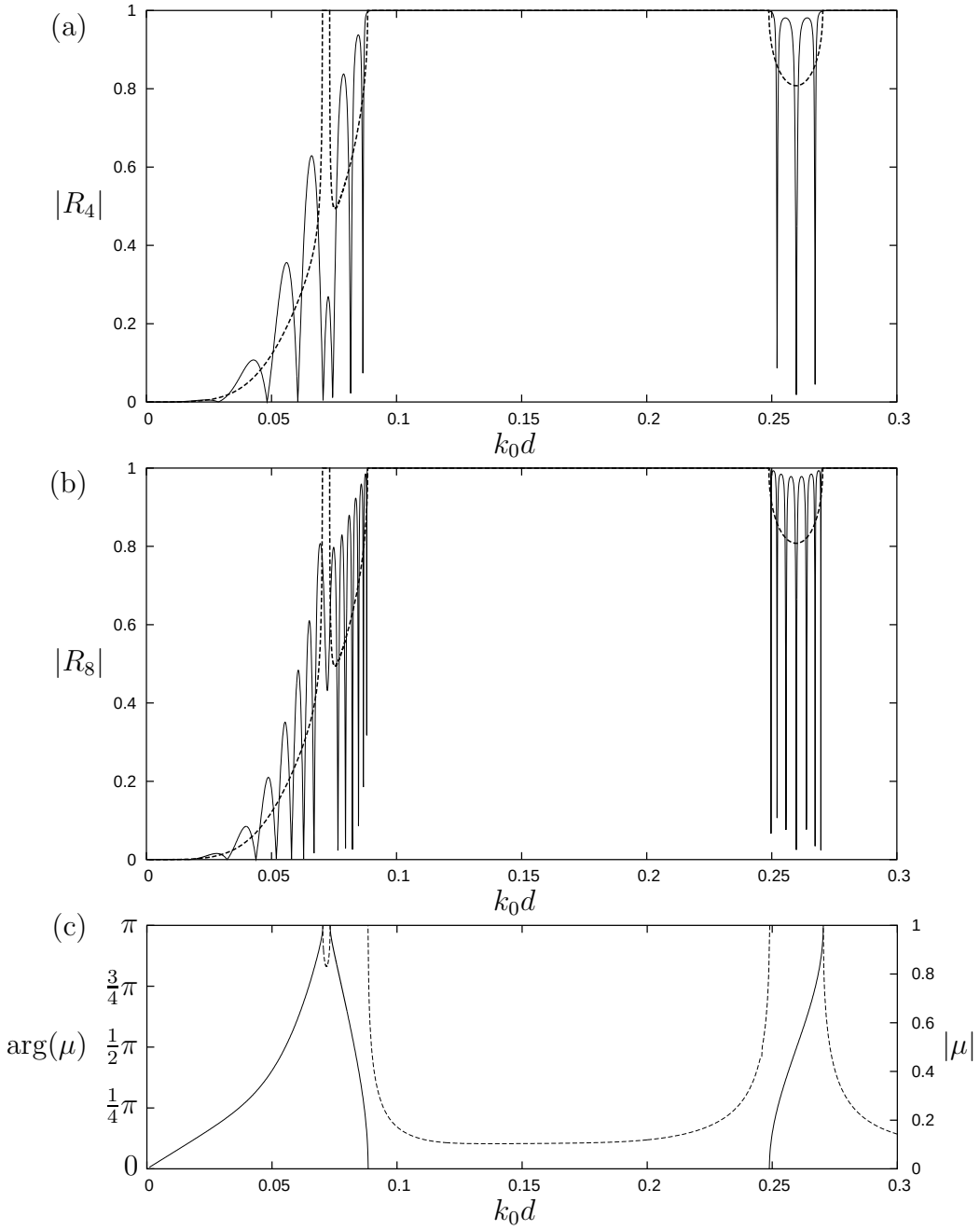

Figure 6: (a) $|R_4|$ and (b) $|R_8|$ against non-dimensional wavenumber k_0d for a crack separation of $b/d = 20$. In both (a) and (b), the bold curve represents $|R_\infty|$ for a semi-infinite periodic array of cracks, $b/d = 20$. In (c) is shown the variation of $\arg(\mu)$ (left-hand scale, solid curve) and $|\mu|$ (right-hand scale, dashed curve) with k_0d for an infinite periodic array of cracks with spacing $b/d = 20$.

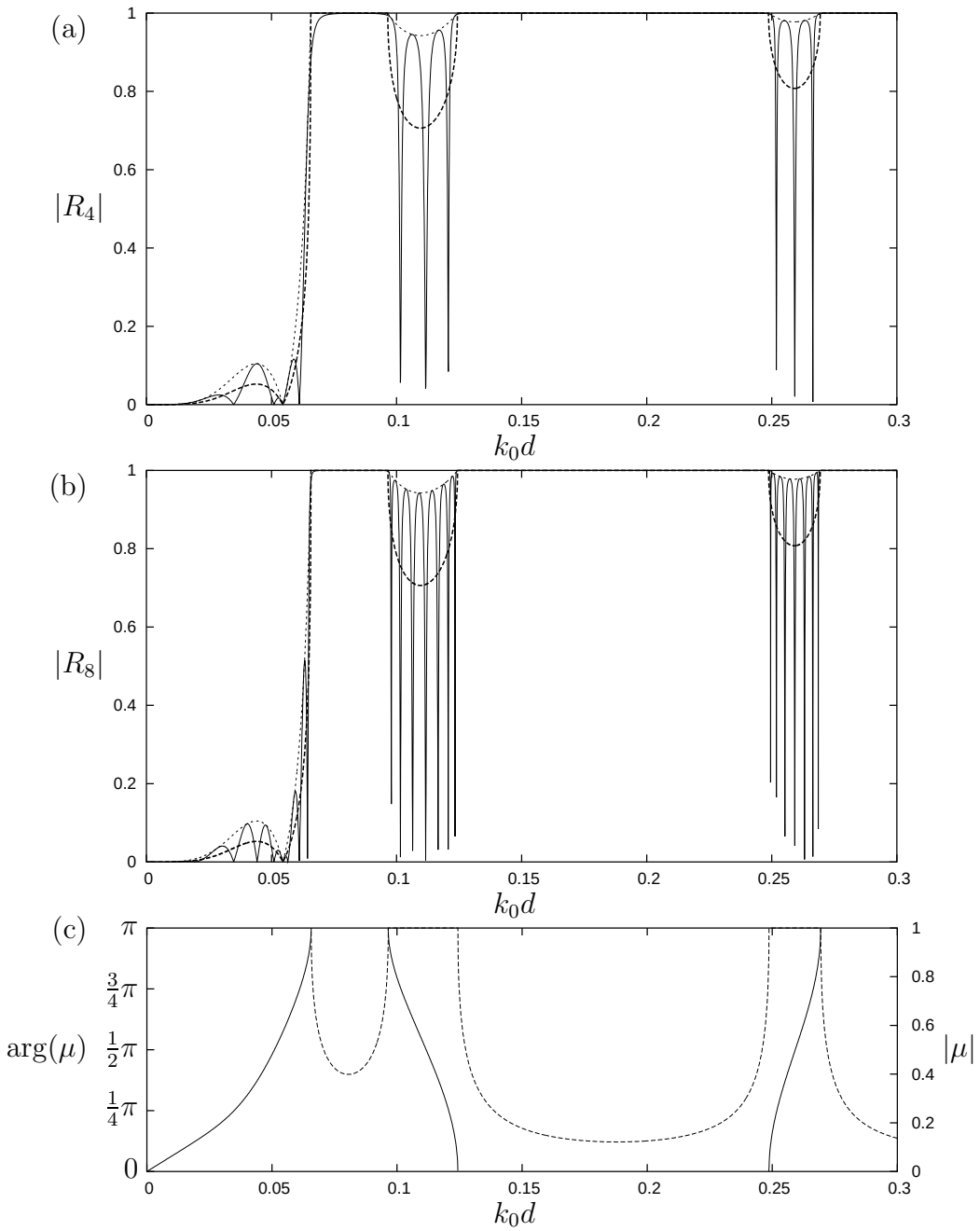

Figure 7: (a) $|R_4|$ and (b) $|R_8|$ against non-dimensional wavenumber k_0d for a crack separation of $b/d = 20$ using the wide-spacing approximation. The bold curve in (a), (b) represents $|R_\infty|$ for a semi-infinite periodic array of cracks, $b/d = 20$, using wide-spacing and the dashed curve is $R_b(k_0)$, the envelope function. In (c) is shown the variation of $\arg(\mu)$ (solid curve, left-hand scale) and $|\mu|$ (dashed curve, right-hand scale) with k_0d based on wide-spacing for an infinite periodic array of cracks with spacing $b/d = 20$.

under the wide-spacing assumption. It turns out, for the exact computations, that if the wrong eigenvalue is chosen then $|R_\infty| > 1$ which clearly cannot occur. Thus, the appropriate eigenvalue can be chosen on the basis that $|R_\infty| < 1$.

A more formulaic basis for the choice of μ is based on the following numerical observation of the behaviour of the particular eigenvalue μ which is needed to calculate R_∞. As $k_0 d$ is increased from zero, μ moves, starting from the real axis, anticlockwise around the complex unit circle until $\mu = -1$. As $k_0 d$ is increased further, μ moves first inwards towards the origin along the real axis and then back out to $\mu = -1$ before continuing around the complex unit circle in anticlockwise fashion. It reaches $\mu = 1$ and again moves back and forth along the real axis with $\mu \leq 1$. This cycle is repeated as $k_0 d$ continues to increase further.

In figure 7 we repeat the calculations made to produce the exact results in figure 6 using the wide-spacing approximation. This is a far simpler task, relying only upon the scattering properties of a single crack. Thus, we are able to calculate $|R_N|$ for $N = 4$ and $N = 8$ in figures 7(a) and (b) respectively using (5.4) and also include the corresponding reflection coefficient for a semi-infinite array of cracks, $|R_\infty|$, calculated using the simple equation (5.5). In addition, the function $R_b(k_0)$ given by (5.7) provides an upper bound on $|R_N|$ independently of the value of N and this is represented in figures 7(a) and (b) by the dashed curves. The wide-spacing results for $|R_N|$ and $|R_\infty|$ relied upon the determination of μ defined as the solution of (5.6) and whose character determines wave propagation in an infinite periodic array. Thus, it is the wide-spacing analogue of the Bloch eigenvalue previously discussed in relation to figure 6(c) and whose behaviour is presented in figure 7(c).

The two sets of figures 6 and 7 allow us to compare directly between the exact and wide-spacing results for periodic arrays of cracks. As expected, the wide-spacing results are in good agreement for $k_0 d \gtrsim 0.2$, corresponding to $\lambda_0/d \lesssim 30$ but do not capture the behaviour of the reflection coefficient for smaller values of $k_0 d$.

7 Wave trapping by two pairs of cracks

It was shown in the results for the scattering of waves by a pair of cracks which are sufficiently closely spaced that zeros of transmission exist at particular frequency (see figures 4 and 5). We pursue this idea in this section by considering an arrangement of two pairs of such closely-spaced cracks and construct solutions which correspond to waves that are trapped on the sheet between the two pairs of cracks. It is easy to argue why such a solution might exist by supposing that the separation between pairs of cracks is large compared to the wavelength. Then, ignoring decaying wave effects, a propagating wave is simply reflected back and forth between the pairs of cracks provided the spacing is chosen to match the phases of the reflected waves at each pair of cracks. Similar arguments have been used to motivate the search for trapped waves by a number of authors (e.g. Linton & Kuznetsov 1997, Porter 2002). More formally, when there is total reflection, $R_2 = \mathrm{e}^{2\mathrm{i}\chi}$ for a pair of cracks located at $x = 0$ and $x = b$ in isolation. Thus, far enough to the left of $x = 0$, we may write $\phi(x, y) \sim (\mathrm{e}^{\mathrm{i}k_0 x} + R_2 \mathrm{e}^{-\mathrm{i}k_0 x}) X_0(y)$. Imposing the condition $\phi_x(-a, y) = 0$, $-h < y < 0$ is equivalent to seeking a symmetric solution about $x = -a$ with another pair of cracks placed at $x = -2a$ and $x = -2a - b$. Alternatively, imposing $\phi(-a, y) = 0$, $-h < y < 0$ presumes a corresponding antisymmetric trapped wave is being sought. Both cases are encapsulated in

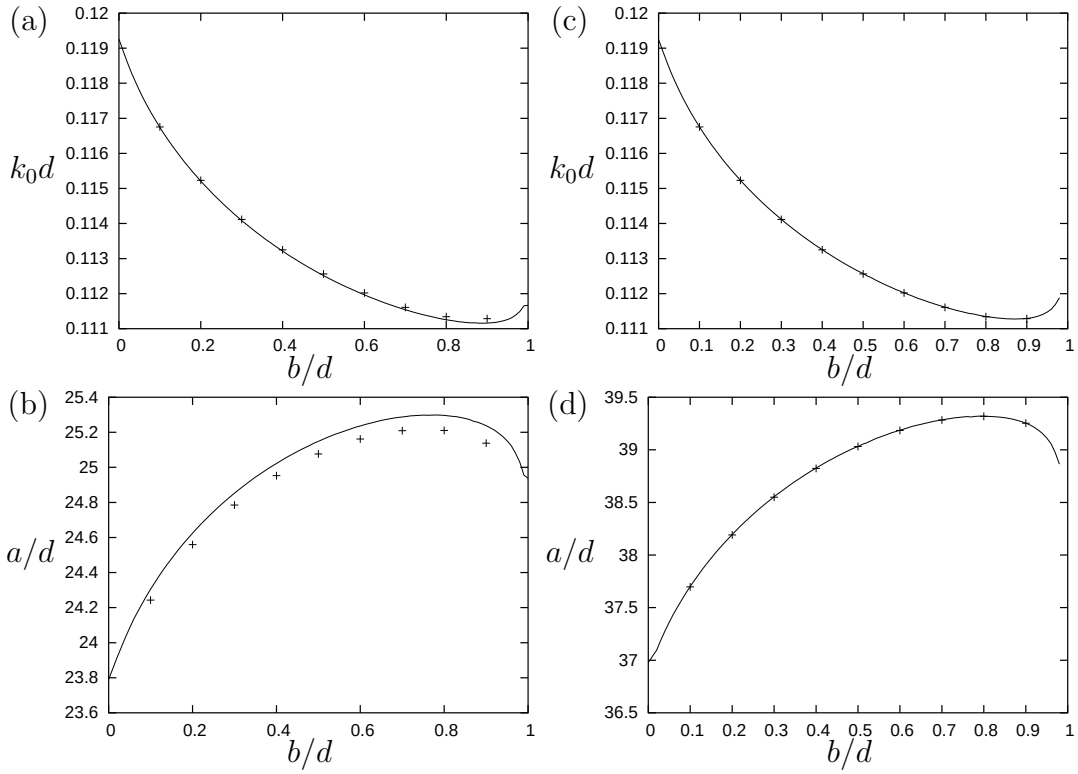

Figure 8: Values of non-dimensional wavenumber, k_0d, and pair separation, a/d, as b/d varies: exact results (solid curves) and wide-spacing approximation (points). In (a) and (b) are the results are for the first symmetric mode ($n = 2$) and in (c) and (d) are the results for the first antisymmetric mode ($n = 3$).

the following result,

$$k_0 a = \frac{1}{2} n\pi - \chi \tag{7.1}$$

where n is taken to be an even integer for symmetric, and an odd integer for antisymmetric, trapped waves. This condition determines an approximation to the half-spacing, a, between the pairs of cracks which has ignored local wave effects.

In order to accurately determine trapped waves, we return to our exact system of equations in (2.54) and (2.55) with $N = 4$ and set the left-hand side terms to zero (since there is now no incident wave forcing the motion). We must then determine values of k_0 and a for a given pair-spacing, b, at which the homogeneous system of equations has non-trivial solutions (alternatively, when the complex-valued determinant of the corresponding 8×8 matrix of coefficients vanishes). Numerically this can be done by using the estimates provided by (7.1) for k_0 and a as initial values in a Newton-Rhapson iterative scheme which tries to find values of k_0 and a where the real and imaginary parts of the determinant are simultaneously zero.

The results are shown in figure 8 where the solid curves represent the results computed from the exact formulation and the points are the corresponding wide-spacing results based on (7.1). Figures 8(a) and (b) show how the non-dimensional wavenumber k_0d and the separation between the pairs of cracks a/d vary as the spacing between each pair of cracks is varied corresponding to the value of $n = 2$ in (7.1); that is the first symmetric mode. As

stated previously in the discussion of figure 4, zeros of transmission for a pair of cracks in isolation occur for $b/d \lesssim 1$ and correspondingly, trapped waves also only occur within this range of values. Figures 8(c) and (d) show similar results for the first antisymmetric trapped mode, by taking $n = 3$ in (7.1). It can be seen that the wide-spacing formula (7.1) is far more accurate than in the first case since the pair of cracks are more widely separated here. Further sets of curves can be produced by taking values of $n \geq 4$.

8 Edge waves supported by multiple cracks

It was shown in EP that for a single crack in an ice sheet, edge waves exist. Edge waves are waves that are local to, and propagating along, the crack but not radiating waves away to infinity perpendicular to the crack. For a configuration consisting of multiple cracks it is also possible to consider edge wave solutions.

In the problem of wave reflection by multiple cracks where the longshore wavenumber l is prescribed in terms of the incident wave angle θ and wavenumber γ_0 by $l = \gamma_0 \sin\theta$. In contrast, for edge waves l is a free parameter and it is usual to seek values of $\gamma_0 < l$ and is no longer possible to progressive waves as $x \to \pm\infty$. The corresponding frequency $\omega(\gamma_0)$ is said to be below the cut-off frequency, $\omega_c = \omega(l)$ where ω is related to the wavenumber via the dispersion relation (2.13).

In order to formulate the edge wave problem, we simply go to (2.54) and (2.55), discarding the terms on the right-hand sides of these equations to reflect the fact that no incident waves are present and interpret the problem with $l > \gamma_0$. In this case, k_0 is now pure imaginery, as fact which allows us to show that s_{jr} and s''_{jr} are pure imaginery whilst s'_{jr} is purely real. A direct consequence of this is that the $2N \times 2N$ determinant formed by the matrix multiplying the coefficients Q_j and P_j on the left-hand side of (2.54) and (2.55) is purely real. Edge wave solutions correspond to the vanishing of this real determinant.

It is possible to draw some conclusions directly from the form of these equations. In particular, d_{jr} is simply the distance between the i-th and j-th crack and if this is sufficiently large we have

$$s_{jr} = s\delta_{jr}, \quad s'_{jr} = s'\delta_{jr}, \quad s''_{jr} = s''\delta_{jr}, \tag{8.1}$$

where s, s' and s'' are obtained by replacing the exponentials in the definition of s_{jr}, s'_{jr} and s''_{jr} (respectively) by unity and have previously been defined in (6.3). It follows that the condition for edge waves now reduces to the equations

$$\left.\begin{aligned} Q_r s' + \mathrm{i} P_r s = 0 \\ Q_r s'' + \mathrm{i} P_r s' = 0 \end{aligned}\right\} \tag{8.2}$$

for $r = 1, 2, \ldots, N$. But in (6.3) it is shown that $s' = 0$ on account of the identity (2.41) so the conditions reduce to

$$Q_r s'' = P_r s' = 0 \tag{8.3}$$

for $r = 1, 2, \ldots, N$. It was also shown in EP that the condition for there to be a symmetric (antisymmetric) edge wave along a single crack was the vanishing of s' (s'') so we see that for sufficiently wide spacing between cracks the condition for edge waves in the presence of N cracks, reduces simply to that for N separate cracks as would be expected, there being no interaction between adjacent cracks.

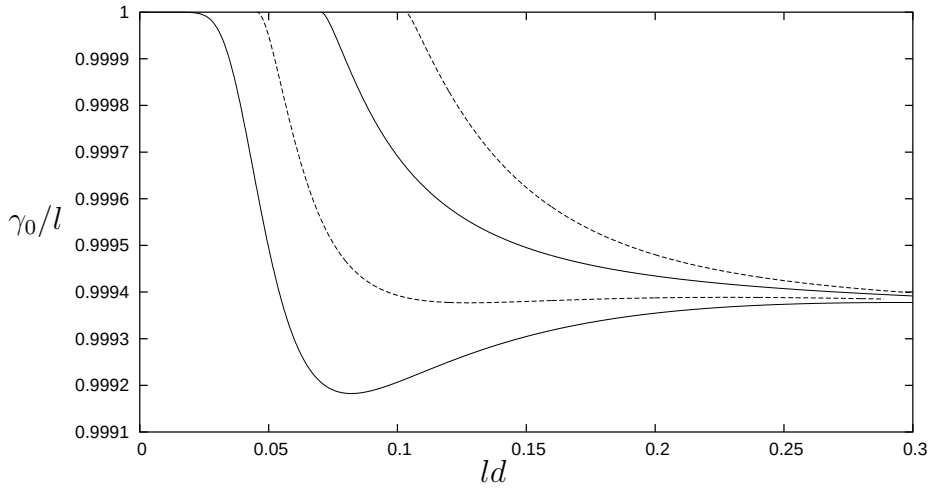

Figure 9: Dispersion curves for edge wave solutions for $N = 4$ cracks equally-separated by $b/d = 500$. Solid and dashed curves represent symmetric and antisymmetric modes respectively.

Results showing the variation of γ_0 with varying non-dimensional longshore wavenumber ld are shown in figure 9 for $N = 4$ cracks of equal spacing given by $b/d = 500$. As noted in EP, the edge wave frequencies occur very close to the cut-off ($\gamma_0 = l$) and so we have plotted curves of γ_0/l against ld. The first thing to notice is that as ld increases (corresponding to a decreasing wavelength along the crack) the four curves tend to the same value, being the edge wave solutions for a single crack in isolation. As ld is decreased, each of the four curves disappears across the cut-off $\gamma_0 = l$. It is possible to identify the modes of oscillation of this symmetrical crack arrangement which are seen to alternate between symmetric and antisymmetric about the centreplane of the configuration.

In figure 10 we show how the edge wave frequencies vary as the spacing between the four equally-spaced cracks is varied, now for a fixed value of $ld = 0.12$. As the spacing between the cracks is increased, the curves all tend to the same value, being the edge wave frequency for a single crack in isolation and as the spacing is reduced the all but one of the solutions disappear through the cut-off.

9 Conclusions

In this paper, the scattering of a train of flexural-gravity waves progressing along an elastic ice sheet resting on the surface of a fluid by an arbitrary number, N, of straight parallel cracks has been considered. By deriving a pair of canonical source functions for a single crack we have been able to demonstrate that the solution for N cracks is expressed simply as a linear combination of these source functions over each crack in terms of a set of $2N$ coefficients which relate to the jumps in elevation and gradient across each crack. These coefficients are determined by the solution of a simple system of $2N$ linear equations and are then used to calculate the reflection and transmission coefficients.

The fact that the solution for N cracks can be expressed both simply and exactly has allowed us to consider extensions to the general scattering problem. Specifically, we have shown that the wave propagation in an infinite periodic array of cracks (the Bloch problem)

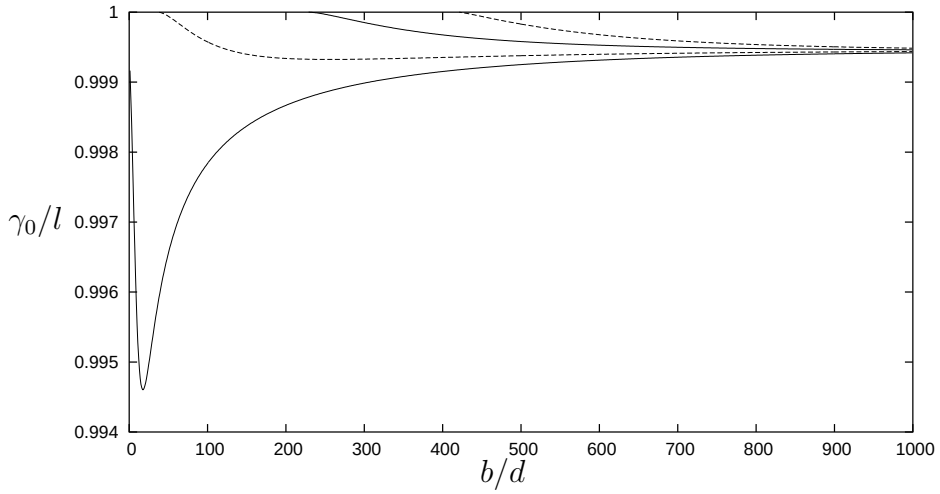

Figure 10: Dispersion curves for edge wave solutions for $N = 4$ cracks equally-separated by b/d and for a fixed value of $ld = 0.12$. Solid and dashed curves represent symmetric and antisymmetric modes respectively.

is governed by the satisfaction of a simple algebraic condition from which a Bloch eigenvalue parameter, μ, is determined. This parameter is then shown to play a key role in formulating the problem of the reflection of waves by a semi-infinite periodic array, which is done exactly in terms of an infinite system of equations and in such a way that the truncated numerical solution converges rapidly.

The wide-spacing approximation has also been developed for the scattering by finite and semi-infinite arrays of cracks where the dependence on the wide-spacing analogue of the Bloch eigenvalue μ for an infinite periodic array is shown to be explicit.

The results for a pair of cracks has shown that, for a small enough crack separation, zeros of transmission exist. This has motivated the search for trapped waves between two pairs of cracks. These two-dimensional trapped waves are distinct from the edge wave solutions that we have also considered which lie below the cut-off frequency. In this case it is shown that, provided the separation between the cracks is large enough, there are as many edge wave solutions as there are cracks. However, edge wave frequencies are located very close to the cut-off in all cases.

A more detailed investigation is needed to fully explain the occurrence of zeros of transmission in the case of two closely-spaced cracks. A further extension of the work here, which takes advantage of the exact solution to the problem, is to consider scattering by arrays of randomly-spaced cracks in which localisation effects would be anticipated.

References

[1] Ashcroft, N. W. & Mermin, N. D. 1976. *Solid State Physics.* W. B. Saunders, Philadelphia.

[2] Botten, L.C., Nicorovici, N.A., McPhedran, R.C., Martin de Sterke, C. & Asatryan, A.A., 2001. Photonic band structure calculations using scattering matrices. *Phys. Rev. E.*, **64**, 046603.

[3] Chamberlain, P.G. & Porter, D. 1995. Decomposition methods for wave scattering by topography with application to ripple beds. *Wave Motion*, **22**, 201–214.

[4] Chou, T. 1998. Band structure of surface flexural-gravity waves along periodic interfaces. *J. Fluid Mech.* **369**, 333–350.

[5] Evans, D.V. & Porter, R., 1997. Trapped modes about multiple cylinders in a channel. *J. Fluid Mech.* , **339**, 331–356.

[6] Evans, D.V. & Porter, R., 2003. Wave scattering by narrow cracks in ice sheets floating on water of finite depth. *J. Fluid Mech.* **484**, 143–165.

[7] Fox, C. & Squire, V.A., 1994. On the oblique reflexion and transmission of ocean waves from the shore fast sea ice. *Phil. Trans. R. Soc. A* **347**(1682), 185–218.

[8] Kriegsmann, G.A., 2003. Scattering matrix analysis of a photonic Fabry-Perot resonator. *Wave Motion*, **37**, 43–61.

[9] Kyriazidou, C.A, Contopangos, H.F., Merill, W.M. & Alexopoulos, N.G., 2000. Artificial versus natural crystals: effective wave impedance of printed photonic bandgap materials. *IEEE Trans. Antennas Propagation*, **48**, 95–105.

[10] Lawrie, J.B. & D. Abrahams, D., 2002. On the propagation and scattering of fluid-structural waves in a three-dimensional duct bounded by thin elastic walls. *Proc. IUTAM Symp. Manchester, UK.* Kluwer Academic Publishers, 279–288.

[11] Leppington, F.G., 1978. Acoustic scattering by membranes and plates with line constraints. *J. Sound Vib.*, **58**(3), 319–332.

[12] Linton, C.M. & Kuznetsov, N.G., 1997. Non-uniqueness in two-dimensional water wave problems: numerical evidence and geometrical restrictions. *Proc. Royal Soc. Lond. A*, **453**, 2437–2460.

[13] McIver, P., 1985. Scattering of water waves by two surface-piercing barriers. *IMA J. Appl. Math.* , **35**, 1–17.

[14] Newman, J.N., 1965. Propagation of water waves past long two-dimensional obstacles. *J. Fluid Mech.* **23**, 23–29.

[15] Nishimoto, M. & Ikuno, H., 1999 Analysis of electromagnetic wave diffraction by a semi-infinite strip grating and evaluation of end-effects. *Progress in Electromagnetic Res.* **23**, 39–58.

[16] Porter, R. & Porter, D. 2003. Scattered and free waves over periodic beds. *J. Fluid Mech.* **483**, 129–163.

[17] Porter, R. & Evans, D.V., 1995. Complementary approximations to wave scattering by vertical barriers *J. Fluid Mech.* , **294**, 155–180.

[18] Squire, V.A. & Dixon A.W., 2001. How a region of cracked sea ice affects ice-coupled wave propagation. *Ann. Glaciol.*, **33**, 327–332.

[19] Squire, V.A., Dugan, J.P., Wadhams, P., Rottier, P.J., & Liu, A.K., 1995. Of ocean waves and ice sheets. *Ann. Rev. Fluid Mech.* , **27**, 115–168.